Available online at www.sciencedirect.com
ScienceDirect
Archives of Biochemistry and Biophysics 465 (2007) 231–246
ABB
www.elsevier.com/locate/yabbi

Inhibition of the two-subsite β-D-xylosidase from *Selenomonas ruminantium* by sugars: Competitive, noncompetitive, double binding, and slow binding modes

Douglas B. Jordan *, Jay D. Braker

Fermentation Biotechnology Research Unit, National Center for Agricultural Utilization Research, U.S. Department of Agriculture, Agricultural Research Service, 1815 North University Street, Peoria, IL 61604, USA

Received 17 April 2007, and in revised form 16 May 2007
Available online 8 June 2007

Abstract

The active site of the GH43 β-xylosidase from *Selenomonas ruminantium* comprises two subsites and a single access route for ligands. Steady-state kinetic experiments that included enzyme (E), inhibitory sugars (I and X) and substrate (S) establish examples of EI, EII, EIX, and EIS complexes. Protonation states of catalytic base (D14, pK_a 5) and catalytic acid (E186, pK_a 7) govern formation of inhibitor complexes and strength of binding constants: e.g., EII, EIX, and EIS occur only with the $D14^{-}E186^{H}$ enzyme and D-xylose binds to $D14^{-}E186^{-}$ better than to $D14^{-}E186^{H}$. Binding of two equivalents of L-arabinose to the $D14^{-}E186^{H}$ enzyme is differentiated by the magnitude of equilibrium K_i values (first binds tighter) and kinetically (first binds rapidly; second binds slowly). In applications, such as saccharification of herbaceous biomass for subsequent fermentation to biofuels, the highly efficient hydrolase can confront molar concentrations of sugars that diminish catalytic effectiveness by forming certain enzyme-inhibitor complexes.
Published by Elsevier Inc.

Keywords: Glycoside hydrolase; GH43; α-L-Arabinofuranosidase; Hysteresis; Hemicellulose; Saccharification; Structure–function

B-D-Xylosidase/α-L-arabinofuranosidase from *Selenomonas ruminantium* (SXA[1]; EC 3.2.1.37 and EC 3.2.1.55) is a bifunctional enzyme of glycoside hydrolase family 43 (GH43) [1–5]. The enzyme is a highly efficient catalyst for promoting hydrolysis of β-1,4-xylooligosaccharides to D-xylose constituents, and its kinetic parameters (k_{cat} and k_{cat}/K_m) exceed those reported for β-xylosidases isolated from other species by 10-fold or greater [3]. In combination with the activities of xylanases, which catalyze hydrolysis of β-1,4 linkages of long polymers of xylose (xylan, a major component of hemicellulose and one of the most abundant biopolymers) to smaller xylooligosaccharides, and other enzymes, which catalyze hydrolysis of acid and sugar substitutions to the C2 and C3 positions of xylose that can occur in xylan depending on its species origin [6–9], SXA has potential utility in processes for saccharification of herbaceous biomass to simple sugars that can be fermented to bioproducts such as bioethanol [10,11].

A common structural feature of GH43 enzymes is a 5-bladed β-propeller domain that comprises the catalytic acid and the catalytic base [12–14]. Recently determined X-ray structures of GH43 β-xylosidases from *Bacillus subtilis*, *Bacillus halodurans*, *Clostridium acetobutylicum*, and *Geobacillus stearothermophilus*, which have 53–70% protein sequence identity with SXA, show that the enzymes possess an additional C-terminal β-sandwich domain that serves to restrict the active site to two subsites with a single route of access for small molecules such as substrate (depicted schematically in Fig. 1) [3,12]. Complementary to the structural

* Corresponding author. Fax: +1 309 681 6427.
E-mail address: douglas.jordan@ars.usda.gov (D.B. Jordan).

[1] *Abbreviations used:* SXA, β-D-xylosidase/α-L-arabinofuranosidase from *Selenomonas ruminantium*; 4NPA, 4-nitrophenyl-α-L-arabinofuranoside; 4NPX, 4-nitrophenyl-β-D-xylopyranoside; GH, glycoside hydrolase; GH43, glycoside hydrolase family 43.

0003-9861/$ - see front matter Published by Elsevier Inc.
doi:10.1016/j.abb.2007.05.016

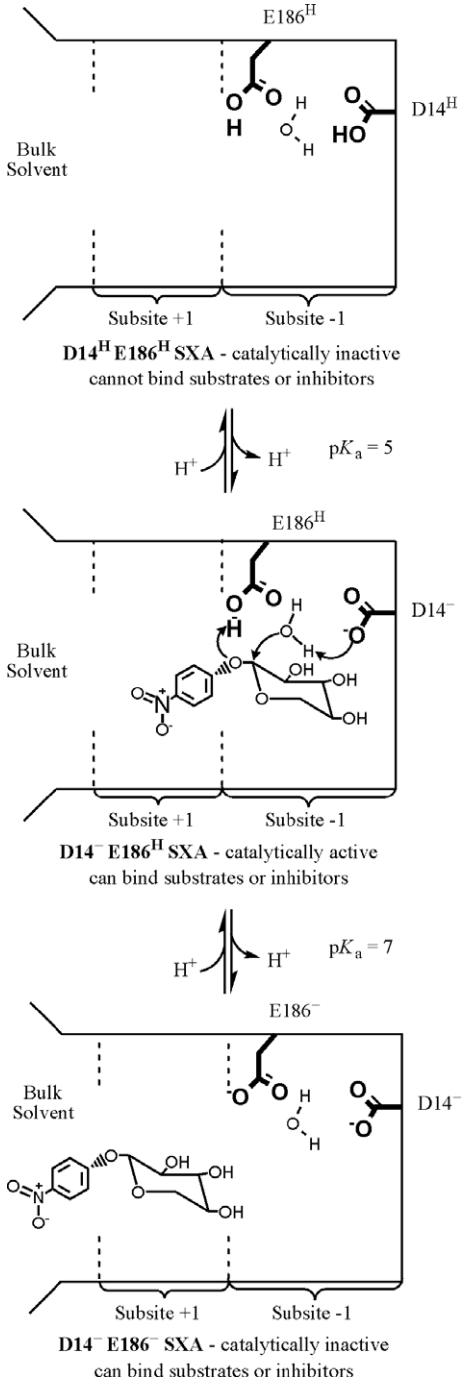

Fig. 1. Schematic model of the SXA active site. The active site comprises two subsites for binding substrates: subsite −1 for the substrate residue at the nonreducing end of substrate and subsite +1 for the first substrate residue on the reducing side of the scissile bond. The catalytically active form of SXA ($D14^{-}E168^{H}$) binds substrate 4NPX so that the catalytic base (D14) and the catalytic acid (E186) can act on the glycosidic bond of hydrolysis. The negative charge of subsite −1 within the catalytically inactive form of SXA ($D14^{-}E168^{-}$) repels 4NPX from binding and the xylose moiety binds to subsite +1 or a portion thereof. The catalytically inactive $D14^{H}E168^{H}$ form of SXA (pK_a 5 for D14) does not bind substrates.

information, biochemical studies have secured that (1) SXA catalyzes hydrolysis of 4NPX and xylobiose with inversion of stereochemistry implicating a single transition state with the catalytic base (D14) serving to activate a water molecule for addition to substrate and the catalytic acid (E186) serving to protonate the leaving group, (2) SXA catalyzes the hydrolysis of a single residue from the nonreducing end of substrate without processivity so that all products of the hydrolysis reaction are removed from the active site before initiating another catalytic cycle, and (3) the β-xylosidase and α-arabinofuranosidase activities share the single active site of the SXA protomer [3].

Interestingly, whereas the pH profiles of kinetic parameter k_{cat}/K_m for substrates 4NPA and 4NPX are similar bell-shaped curves governed by $pK_a \sim 5$ for the acidic limb (assigned to SXA catalytic base D14) and by $pK_a \sim 7$ for the basic limb (assigned to SXA catalytic acid E186), the pH profiles for k_{cat} differ between the two substrates: both substrates have a drop in k_{cat} on the acid side with $pK_a \sim 3.5$ (perturbed from $pK_a \sim 5$ by increases in K_m for both substrates), but k_{cat}(4NPX) drops on the basic side ($pK_a \sim 7$), whereas k_{cat}(4NPA) remains flat at its pH-independent value beyond pH 8. Differences between the substrates' pH profiles for k_{cat} at alkaline pH are reflected in the pH profiles for $1/K_m$: the pH dependency for $1/K_m$(4NPA) is described by a bell-shaped curve with $pK_a \sim 5$ for the acidic limb and $pK_a \sim 7$ for the basic limb, whereas that for $1/K_m$(4NPX) is described by two acidic limbs with pK_a values of 5 and 7 [3]. The differences have been interpreted in terms of three protonation states of SXA: the catalytically inactive, diprotonated $D14^{H}E186^{H}$ enzyme in which the catalytic base and catalytic acid are both protonated, binds neither 4NPA nor 4NPX; the catalytically active monoprotonated $D14^{-}E186^{H}$ enzyme which can bind both substrates; and catalytically inactive deprotonated $D14^{-}E186^{-}$ enzyme, which can bind 4NPX (nonproductively) but cannot bind 4NPA. As depicted schematically in Fig. 1, it was further postulated that the negatively charged active site of $D14^{-}E186^{-}$ SXA repels the xylose moiety of 4NPX from binding fully in subsite −1 (as it would in the productive complex with $D14^{-}E186^{H}$ SXA) so that it moves to occupy a portion of subsite +1 [3].

In this work, we set out to expand the limited binding information on SXA to include binding of commonly occurring sugars and glycosides, some of which (e.g., L-arabinose, D-xylose and D-glucose) can be expected to approach concentrations of 0.3–3 M in saccharified biomass. In the context of the two-subsite model of SXA, potential inhibitory complexes of SXA interacting with two inhibitors are defined in Scheme 1, which allows for random binding of ligands except for the case of an enzyme complex containing substrate (or any other ligand that would occupy both subsites −1 and +1) and a monosaccharide (EIS) in which the monosaccharide must bind first; because if substrate bound first then both subsites would be occupied leaving no vacancy for the monosaccharide; thus there are requirements for ordered addition to the SXA active site which has a single route for entry and exit. Even though SXA exists as a homotetramer, active sites are far

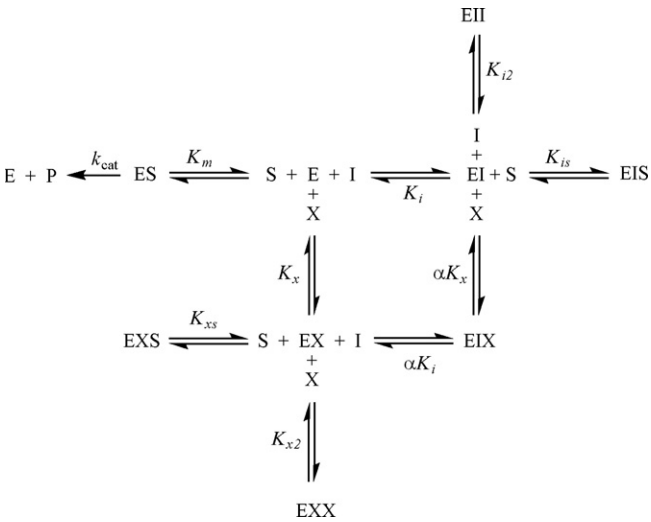

Scheme 1. Binding of two inhibitors (I and X) and substrate (S) to the two-subsite SXA (E). P is product and *K*s are dissociation constants. Based on X-ray structures of GH43 β-xylosidases, whose active site comprises two subsites with access limited to one side (as shown in schematic of Fig. 1) of the active site, the scheme shows ordered binding of inhibitor before substrate because if the substrate were to bind first, it would occupy both subsites −1 and +1 or subsite +1 and there would be no space for the inhibitor to bind or there would be no access to subsite −1.

apart from one another and each comprises residues belonging entirely to the same monomer. As well, there is no evidence for cooperativity in substrate saturation curves, and X-ray structures of GH43 β-xylosidases from *Geobacillus stearothermophilus* indicate no gross differences between active sites of free enzyme and enzyme complexed with substrate xylobiose. Therefore, the model does not encompass cooperative binding of inhibitors.

Materials and methods

Materials and general methods

4NPA, 4NPX, inhibitor candidates, and buffers were obtained from Sigma-Aldrich. Water was purified through a Milli-Q unit (Millipore). All other reagents were reagent grade and high purity. A Cary 50 Bio UV–Visible spectrophotometer (Varian), equipped with a thermostatted holder for cuvettes, was used for spectral and kinetic determinations. A model SX.18MV-R stopped-flow (Applied Photophysics) with a thermostatted compartment for syringes and reaction chamber and a 2 mm path length for absorbance measurements was used for rapid kinetic studies. SXA was cloned from *S. ruminantium*, and expressed in *Escherichia coli* [2]. SXA was purified to homogeneity (judged by SDS-PAGE analysis) as described [3], with the addition of a final desalting, gel filtration step employing a 2.6 × 30 cm column of Bio-Gel P-6 DG desalting gel (Bio-Rad), equilibrated and eluted with 20 mM sodium phosphate, pH 7.0.

Enzyme reactions

Unless indicated otherwise, reactions were initiated by adding a small aliquot of enzyme (generally 7 μL of enzyme diluted into 10 mM sodium phosphate, pH 7.0, and incubated on wet ice or at ∼25 °C) to 1-mL, temperature-equilibrated (25 °C) reaction mixtures, which were monitored continuously (Cary spectrophotometer) for 0.3 min at 380 nm (for pH values below 6) or 400 nm (for pH values of 6 and above) for determinations of linear initial rates (steady-state rates). Time required for enzyme addition and mixing was 0.2 min prior to collection of rate data. With 4NPA and 4NPX, initial rates determined from 0.1-s (using stopped-flow instrument) and 30-min reactions were similar [3]. Described methods were employed for determinations of delta extinction coefficients (product − substrate) used for molar conversion for each reaction condition and for end point determinations of 4NPA and 4NPX substrate concentrations [3]; these determinations relied on the reported extinction coefficient of 18.3 $mM^{-1}\,cm^{-1}$ at 400 nm for 4-nitrophenol in NaOH [15]. Buffers of constant ionic strength ($I = 0.3$ M), adjusted with NaCl, in the complete reaction mixtures were used as indicated: 100 mM succinate–NaOH (pH 4.3–6), 100 mM sodium phosphate (pH 6–8), 30 mM sodium pyrophosphate (pH 8–10). Values for v and k_{cat} are expressed in moles substrate hydrolyzed per second per mole of enzyme active sites (protomers), the latter calculated from the calculated extinction coefficient of SXA protomers at 280 nm of 129,600 $M^{-1}\,cm^{-1}$ [3,16]. Details of reaction conditions for lag and burst experiments are described in the figure legends.

Equations

Data were fitted to equations using the computer program Grafit (Erithacus Software) [17]. Simple weighting (constant error) was used for fitting most data; proportional error weighting was used to fit some data (e.g., certain pH curves). Most symbol definitions for Eqs. (1)–(13) are defined by Scheme 1: v is the observed initial (steady-state) rate of catalysis, k_{cat} is the maximum rate of catalysis, S is the substrate concentration, K_m is the Michaelis constant, I and X are the inhibitor concentrations, K_i is the dissociation constant for I from EI, K_x is the dissociation constant for X from EX, αK_i is the dissociation constant for I from EIX, αK_x is the dissociation constant for X from EIX, K_{i2} is the dissociation constant for I from EII, K_{x2} is the dissociation constant for X from EXX, and K_{is} is the dissociation constant for S from EIS; K_{is} should not be confused with its more common usage in enzyme kinetics as representing the inhibition constant for k_{cat}/K_m. For Eqs. (12) and (13), d is a correction factor for absorbance by the spectrophotometer prior to recording data, v_s is the steady-state rate, v_0 is the initial rate of catalysis, k_{obs} is the first-order rate constant for the burst or lag, and t is the reaction time. $K_{i2(rapid)}$, the dissociation constant for I from EII, and k_{on} and k_{off} are described by Scheme 2. Eq. (1) describes competitive inhibition; Eq. (2), noncompetitive inhibition; Eq. (3), competitive, double binding inhibition; Eq. (4), noncompetitive, double binding inhibition; Eq. (5), competitive, triple binding inhibition; Eq. (6), inhibition by two exclusive, competitive inhibitors; Eq. (7), inhibition by two nonexclusive competitive inhibitors; Eq. (8), inhibition by two exclusive, competitive inhibitors (one double binding); Eq. (9), inhibition by two nonexclusive competitive inhibitors (one double binding); Eq. (10), inhibition by two exclusive competitive inhibitors (both double binding); Eq. (11), inhibition by two nonexclusive competitive inhibitors (both double binding); and Eq. (13), the forward and reverse rates for transforming EII to EII*. These equations are derived in Appendix S1 of Supplementary data.

For Eqs. (14)–(17), p is the determined parameter at a single pH, P is the pH-independent value of the parameter, K_a is the acid dissociation constant of the group affecting P, H^+ is the proton concentration, K_{a1} is the acid dissociation constant of the first group affecting P, K_{a2} is the acid dissociation constant of the second group affecting P, P_1 is the limit of p associated with K_{a1}, and P_2 is the limit of p associated with K_{a2}.

$$v = \frac{k_{cat} * S}{K_m\left(1 + \frac{I}{K_i}\right) + S} \tag{1}$$

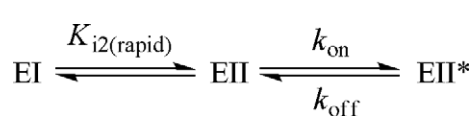

Scheme 2. Slow binding of the second equivalent of L-arabinose.

$$v = \frac{k_{cat} * S}{K_m\left(1 + \frac{I}{K_i}\right) + S\left(1 + \frac{K_m * I}{K_{is} * K_i}\right)} \quad (2)$$

$$v = \frac{k_{cat} * S}{K_m\left(1 + \frac{I}{K_i} + \frac{I^2}{K_i * K_{i2}}\right) + S} \quad (3)$$

$$v = \frac{k_{cat} * S}{K_m\left(1 + \frac{I}{K_i} + \frac{I^2}{K_i * K_{i2}}\right) + S\left(1 + \frac{K_m * I}{K_{is} * K_i}\right)} \quad (4)$$

$$v = \frac{k_{cat} * S}{K_m\left(1 + \frac{I}{K_i} + \frac{I^2}{K_i * K_{i2}} + \frac{I^3}{K_i * K_{i2} * K_{i3}}\right) + S} \quad (5)$$

$$v = \frac{k_{cat} * S}{K_m\left(1 + \frac{I}{K_i} + \frac{X}{K_x}\right) + S} \quad (6)$$

$$v = \frac{k_{cat} * S}{K_m\left(1 + \frac{I}{K_i} + \frac{X}{K_x} + \frac{I * X}{K_i * K_x * \alpha}\right) + S} \quad (7)$$

$$v = \frac{k_{cat} * S}{K_m\left(1 + \frac{I}{K_i} + \frac{X}{K_x} + \frac{I^2}{K_i * K_{i2}}\right) + S} \quad (8)$$

$$v = \frac{k_{cat} * S}{K_m\left(1 + \frac{I}{K_i} + \frac{X}{K_x} + \frac{I^2}{K_i * K_{i2}} + \frac{I * X}{K_i * K_x * \alpha}\right) + S} \quad (9)$$

$$v = \frac{k_{cat} * S}{K_m\left(1 + \frac{I}{K_i} + \frac{X}{K_x} + \frac{I^2}{K_i * K_{i2}} + \frac{X^2}{K_x * K_{x2}}\right) + S} \quad (10)$$

$$v = \frac{k_{cat} * S}{K_m\left(1 + \frac{I}{K_i} + \frac{X}{K_x} + \frac{I^2}{K_i * K_{i2}} + \frac{X^2}{K_x * K_{x2}} + \frac{I * X}{K_i * K_x * \alpha}\right) + S} \quad (11)$$

$$\text{Absorbance} = d + v_s * t + \frac{v_0 - v_s * \left(1 - e^{-k_{obs} * t}\right)}{k_{obs}} \quad (12)$$

$$k_{obs} = k_{off} + \frac{k_{on}}{1 + \frac{K_i * K_{i2(rapid)}}{I^2} + \frac{K_{i2(rapid)}}{I} + \frac{K_{i2(rapid)} * S}{I * K_{is}} + \frac{S * K_i * K_{i2(rapid)}}{K_m * I^2}} \quad (13)$$

$$p = \frac{P}{1 + \frac{H^+}{K_a}} \quad (14)$$

$$p = \frac{P}{1 + \frac{K_a}{H^+}} \quad (15)$$

$$p = \frac{P}{1 + \frac{H^+}{K_{a1}} + \frac{K_{a2}}{H^+}} \quad (16)$$

$$p = \frac{P_1}{1 + \frac{H^+}{K_{a1}}} + \frac{P_2 - P_1}{1 + \frac{H^+}{K_{a2}}} \quad (17)$$

Results and discussion

Inhibition of SXA catalysis by individual sugars and glycosides at pH 7.0

A survey of potential inhibitors of SXA-catalyzed hydrolysis of 4NPX is arranged in order of descending potency from the relative catalytic rates determined in reactions containing 100 mM inhibitor candidate and 1.0 mM 4NPX at pH 7.0 (Table 1; an extended table is Table S1 of Supplementary data). pH 7.0 was chosen for the survey because it is the pK_a assigned to the catalytic acid of SXA (E186) and substrate 4NPX has been shown to bind to both the protonated $E186^H$ (productive enzyme form) and the ionized $E186^-$ (nonproductive enzyme form) [3]. D-Xylose and D-ribose are the most potent inhibitors of the survey and nearly all sugars examined had some affinity for SXA. Promiscuity for glycone inhibitors by the binding pocket of the homologous (62% identical protein sequence as SXA) β-xylosidase from *Bacillus pumilus* is revealed by its similar affinities for inhibitors with glycone moieties locked in the $^4C_1$ and $^1C_4$ conformations [18]. Notably, sucrose does not inhibit SXA catalysis; the compound has been used in molar concentrations to raise the viscosity of SXA reaction mixtures in experiments that ruled out diffusion as a factor controlling SXA catalysis [3]. More detailed analysis of inhibition modes by nine of the inhibitors identified in the survey began with experiments, which held substrates 4NPX and 4NPA at constant, subsaturating concentrations and varied inhibitor concentrations widely to determine stoichiometries of inhibitor molecules per SXA active site. Linear Dixon plots ($1/v$ versus inhibitor concentration) of the inhibition data are indicative of single binding inhibitors, and Dixon plots with upward curvature are diagnostic of multiple inhibitor binding as shown for L-arabinose and D-ribose (Fig. 2). Through Dixon plot analyses and by fitting the inhibition data to Eq. (1) (single binding) and Eq. (3) (double binding) with F test comparisons of the goodness of fit, five of the nine inhibitors were determined to bind SXA with a stoichiometry of 1 and four inhibitors with a stoichiometry of 2 (Table 1). For example, in the case of D-glucose, the F test comparisons indicate 100% probability that the data fit Eq. (1) (no double binding term) as well as Eq. (3) (with double binding term) and the determined K_{i2} values for binding a second equivalent of inhibitor are huge (relative to Ki) and not well determined, whereas in the case of D-ribose, the F test comparisons indicate 0.00% probability that the inhibition data fit Eq. (1) as well as Eq. (3) and the determined values for K_{i2} are well determined and ~ 10-fold the K_i values for binding the first equivalent.

Single binding inhibitors

This group includes cellobiose (4-*O*-β-D-glucopyranosyl-D-glucose), D-glucose, maltose (4-*O*-α-D-glucopyranosyl-D-glucose), D-xylose, and L-xylose. Further analysis of binding modes is from data obtained by varying substrate and inhibitor concentrations, fitting the data to Eq. (1) (competitive inhibition) and Eq. (2) (noncompetitive inhibition) and executing F tests for comparisons (Table 1). With the exceptions of D-xylose and L-xylose, the single-binding inhibitors of SXA were determined to be competitive with respect to the varied substrates 4NPA and 4NPX. In terms of Scheme 1, inhibitors cellobiose, D-glucose, and maltose bind SXA to form EI and fully exclude substrates 4NPA and 4NPX from binding so that EIS cannot form.

D-Xylose is clearly a competitive inhibitor with respect to substrate 4NPA as the F test comparisons of data from experiments 3a and 3b provide 100% probability that the data fit Eq. (1) as well as Eq. (2) and the values for K_{is} determined from fitting the data to Eq. (2) are enormous in comparison to the determined value for K_m(4NPA) of 1.08 mM (Table 1). However, inhibitor D-xylose is

Table 1
Inhibition of SXA catalysis by single sugars and glycosides at pH 7.0 and 25 °C[a]

Inhibitor candidate	(Experiment number)/ [Substrate]	Relative rate at 100 mM inhibitor candidate[b]	K_i (mM)	K_{is} (mM)	K_{i2} (mM)	*F* test probability (%)/preferred equation	Binding mode[c]
Inhibitor free		1.00 ± 0.01					
D-Xylose	(1)/1 mM 4NPX	0.130 ± 0.001					
D-Xylose	(2a)/0.2–5 mM 4NPX		3.79 ± 0.06[d], 4.16 ± 0.08[e]	41.6 ± 6.4[e]		0.00/Eq. (2)	NC, SB
D-Xylose	(2b)/0.2–5 mM 4NPX		3.82 ± 0.06[d], 4.04 ± 0.08[e]	51.0 ± 13.8[e]		0.13/Eq. (2)	NC, SB
D-Xylose	(3a)/0.2–5 mM 4NPA		4.27 ± 0.06[d], 4.27 ± 0.06[e]	10^{25}[e]		100/Eq. (1)	C, SB
D-Xylose	(3b)/0.2–5 mM 4NPA		4.42 ± 0.10[d], 4.42 ± 0.10[e]	10^{20}[e]		100/Eq. (1)	C, SB
D-Xylose ($n = 8$)	(4)/1 mM 4NPA		4.41 ± 0.30[f], 4.44 ± 0.31[g]		10^{25}[g]	100/Eq. (1)	SB
D-Xylose	(5)/1 mM 4NPX		4.19 ± 0.18[f], 4.23 ± 0.37[g]		$(7 \pm 60) \times 10^{3}$[g]	91/Eq. (1)	SB
Methyl β-D-xylopyranoside	1 mM 4NPX	0.152 ± 0.001					
D-Ribose	(1)/1 mM 4NPX	0.158 ± 0.002					
D-Ribose	(2)/0.2–5 mM 4NPX		13.3 ± 1.2[h], 13.3 ± 1.2[i]	10^{25}	83.5 ± 13.7[h], 83.5 ± 14.0[i]	100/Eq. (3)	C, DB
D-Ribose	(3)/0.2–5 mM 4NPA		17.6 ± 2.1[h], 17.6 ± 2.2[i]	10^{17}	91.6 ± 21.9[h], 91.6 ± 22.3[i]	100/Eq. (3)	C, DB
D-Ribose ($n = 7$)	(4)/1 mM 4NPA		8.87 ± 0.58[f], 12.7 ± 1.5[g]		106 ± 14[g]	0.005/Eq. (3)	DB
D-Ribose	(5)/1 mM 4NPX		5.67 ± 0.47[f], 9.48 ± 0.25[g]		118 ± 8[g]	0.00/Eq. (3)	DB
D-Ribose	(6)/0.05 mM 4NPX		8.65 ± 0.51[f], 11.9 ± 0.2[g]		107 ± 6[g]	0.00/Eq. (3)	DB
L-Arabinose	(1)/1mM 4NPX	0.253 ± 0.006					
L-Arabinose	(2)/0.2–5 mM 4NPX		11.2 ± 1.4[h], 17.1 ± 1.0[i]	3.45 ± 0.34[i]	125 ± 37[h], 111 ± 14[i]	0.00/Eq. (4)	NC, DB
L-Arabinose	(3)/0.2–5 mM 4NPA		13.3 ± 1.2[h], 20.3 ± 0.5[i]	5.07 ± 0.23[i]	117 ± 27[h], 86.9 ± 4.2[i]	0.00/Eq. (4)	NC, DB
L-Arabinose ($n = 6$)	(4)/1 mM 4NPA		11.2 ± 1.0[f], 16.9 ± 1.7[g]		118 ± 23[g]	0.05/Eq. (3)	DB
L-Arabinose ($n = 4$)	(5)/0.05 mM 4NPX		13.6 ± 2.1[f], 21.3 ± 2.5[g]		94.4 ± 18.5[g]	0.03/Eq. (3)	DB
D-Erythrose	(1)/1 mM 4NPX	0.261 ± 0.002					
D-Erythrose	(2)/0.2–5 mM 4NPX		9.85 ± 0.5[h], 11.3 ± 0.2[i]	12.5 ± 0.7[i]	888 ± 330[h], 1680 ± 330[i]	0.00/Eq. (4)	NC, DB
D-Erythrose	(3)/0.2–5 mM 4NPA		13.0 ± 0.2[h], 13.3 ± 0.2[i]	118 ± 46[i]	1590 ± 280[h], 1720 ± 320[i]	1.2/Eq. (4)	NC, DB
D-Erythrose	(4)/1 mM 4NPA		13.3 ± 0.3[f], 14.4 ± 0.2[g]		1170 ± 150[g]	0.00/Eq. (3)	DB
D-Erythrose	(5)/1 mM 4NPX		9.94 ± 0.17[f], 10.38 ± 0.13[g]		2620 ± 600[g]	0.15/Eq. (3)	DB
4-Hydroxyphenyl-β-D-glucopyranoside	1 mM 4NPX	0.289 ± 0.004					
L-Xylose	(1) 1 mM 4NPX	0.334 ± 0.005					
L-Xylose	(2a)/0.2–5 mM 4NPX		13.2 ± 0.2[d], 13.4 ± 0.3[e]	166 ± 189[e]		38/Eq. (2)	NC, SB
L-Xylose	(2b)/0.2–5 mM 4NPX		15.8 ± 0.3[d], 16.1 ± 0.4[e]	121 ± 98[e]		22/Eq. (2)	NC, SB
L-Xylose	(3a)/0.2–5 mM 4NPA		12.9 ± 0.2[d], 14.0 ± 0.3[e]	43.5 ± 9.3[e]		0.003/Eq. (2)	NC, SB
L-Xylose	(3b)/0.2–5 mM 4NPA		12.3 ± 0.3[d], 13.0 ± 0.5[e]	64.7 ± 36.3[e]		7.6/Eq. (2)	NC, SB
L-Xylose	(4)/1 mM 4NPA		13.6 ± 0.2[f], 13.6 ± 0.2[g]		10^{27}[g]	100/Eq. (1)	SB
L-Xylose	(5)/1 mM 4NPX		14.3 ± 0.1[f], 14.3 ± 0.2[g]		$10^{13} \pm 10^{14}$[g]	100/Eq. (1)	SB
Methyl-α-D-glucopyranoside	1mM 4NPX	0.423 ± 0.006					
D-Glucose	(1)/1mM 4NPX	0.500 ± 0.004					
D-Glucose	(2a)/0.2–5 mM 4NPX		26.3 ± 0.5[d], 26.3 ± 0.5[e]	10^{18}[e]		100/Eq. (1)	C, SB
D-Glucose	(2b)/0.2–5 mM 4NPX		34.5 ± 0.7[d], 34.5 ± 0.7[e]	10^{25}[e]		100/Eq. (1)	C, SB
D-Glucose	(3)/0.2–5 mM 4NPA		27.0 ± 0.4[d], 27.0 ± 0.4[e]	10^{22}[e]		100/Eq. (1)	C, SB
D-Glucose ($n = 5$)	(4)/1 mM 4NPA		27.0 ± 0.5[f], 27.0 ± 0.5[g]		10^{26}[g]	100/Eq. (1)	SB
D-Glucose	(5)/1 mM 4NPX		30.5 ± 0.6[f], 30.5 ± 0.6[g]		10^{18}[g]	100/Eq. (1)	SB
Maltose	(1)/1 mM 4NPX	0.546 ± 0.007					
Maltose	(2)/0.2–5 mM 4NPX		28.6 ± 0.8[d], 28.0 ± 1.2[e]	10^{14}[e]		100/Eq. (1)	C, SB
Maltose	(3)/0.3–5 mM 4NPA		32.4 ± 0.6[d], 32.4 ± 0.6[e]	10^{26}[e]		100/Eq. (1)	C, SB
Maltose	(4)/1 mM 4NPA		29.6 ± 0.5[f], 30.0 ± 1.2[g]		7550 ± 21200[g]	73/Eq. (1)	SB
Maltose	(5)/1 mM 4NPX		31.0 ± 0.6[f], 31.0 ± 0.6[g]		10^{28}[g]	100/Eq. (1)	SB

(*continued on next page*)

Table 1 (*continued*)

Inhibitor candidate	(Experiment number)/ [Substrate]	Relative rate at 100 mM inhibitor candidate[b]	K_i (mM)	K_{is} (mM)	K_{i2} (mM)	*F* test probability (%)/preferred equation	Binding mode[c]
Melibiose	1 mM 4NPX	0.578 ± 0.001					
Cellobiose	(1)/1 mM 4NPX	0.603 ± 0.024					
Cellobiose	(2)/0.2–5 mM 4NPX		49.8 ± 1.8[d], 49.5 ± 2.5[e]	10^{12}[e]		100/Eq. (1)	C, SB
Cellobiose	(3)/1 mM 4NPA		42.9 ± 0.5[f], 42.9 ± 1.4[g]		220,000[g]	99/Eq. (1)	C, SB
Cellobiose	(4)/1 mM 4NPX		57.1 ± 1.3[f], 57.1 ± 1.4[g]		10^{24}[g]	100/Eq. (1)	SB
D-Galactose	1 mM 4NPX	0.607 ± 0.004					
D-Arabinose	(1)/1 mM 4NPX	0.621 ± 0.001					
D-Arabinose	(2a)/0.2–5 mM 4NPX		57.6 ± 1.9[h], 57.6 ± 1.9[i]	10^{21}	1330 ± 230[h], 1330 ± 230[i]	100/Eq. (3)	C, DB
D-Arabinose	(2b)/ 0.2–5 mM 4NPX		54.8 ± 2.7[h], 54.8 ± 2.7[i]	10^{24}	1370 ± 420[h], 1370 ± 430[i]	100/Eq. (3)	C, DB
D-Arabinose	(3)/ 0.2–5 mM 4NPA		67.1 ± 2.3[h], 67.1 ± 2.3[i]	10^{19}	1550 ± 360[h], 1550 ± 370[i]	100/Eq. (3)	C, DB
D-Arabinose ($n = 5$)	(4)/1 mM 4NPA		58.9 ± 0.8[f], 62.4 ± 1.8[g]		2170 ± 740[g]	2.6/Eq. (3)	DB
D-Arabinose	(5)/1 mM 4NPX		48.9 ± 1.7[f], 57.6 ± 1.1[g]		1590 ± 170[g]	0.01/Eq. (3)	DB
Sucrose	1 mM 4NPX	1.01 ± 0.030					

Standard errors of the fits are indicated. *F* test probabilities compare goodness of fit of data from a single experiment number to two equations; in all cases reported here, the % probability refers to the probability that the data fit the equation with fewer parameters as well as the equation with more parameters—the preferred equation is indicated. When *n* is indicated the determined value is the mean of *n* independent determinations, the error is the standard deviation of the mean, and the *F* test probability is the mean of *n* *F* tests.

[a] Reactions contained 100 mM sodium phosphate, $I = 0.3$ M, pH 7.0 at 25 °C. Substrate concentrations are indicated for each experiment number. Duplicate experiments are shown to emphasize *F* test results. Inhibitor concentrations were varied for all K_i, K_{is}, and K_{i2} determinations; highest concentrations of inhibitor candidates were 150 mM D-xylose, 300 mM D-ribose, 300 mM L-arabinose, 700 mM D-erythrose, 300 mM L-xylose, 300 mM D-glucose, 300 mM maltose, 150 mM cellobiose, 500 mM D-arabinose, and 100 mM for the other inhibitor candidates.

[b] Relative to control rate ($v = 8.64 \pm 0.10\ s^{-1}$) in the absence of inhibitor. For determination of relative rates, reactions contained 100 mM inhibitor candidate and 1.0 mM 4NPX; under these conditions, K_m(4NPX) = 0.38 mM. Means and standard deviations of at least 2 replicates are indicated.

[c] Conclusions based on preferred equation: C, competitive (forms EI); NC, noncompetitive (forms EI and EIS); SB, single binding; DB, double binding.

[d] Initial-rate data were fitted to Eq. (1).

[e] Initial-rate data were fitted to Eq. (2).

[f] Initial-rate data were fitted to Eq. (1) with constant values for K_m(4NPA) = 1.08 mM and K_m(4NPX) = 0.38 mM.

[g] Initial-rate data were fitted to Eq. (3) with constant values for K_m(4NPA) = 1.08 mM and K_m(4NPX) = 0.38 mM.

[h] Initial-rate data were fitted to Eq. (3).

[i] Initial-rate data were fitted to Eq. (4).

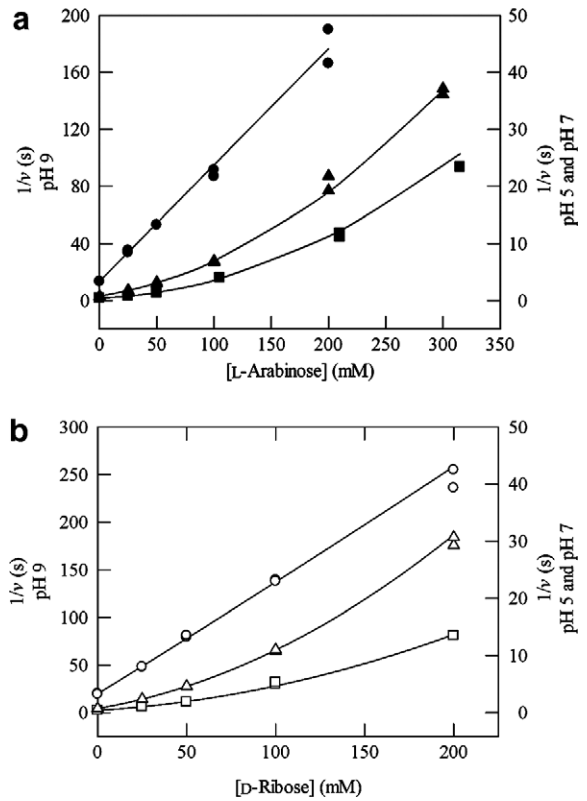

Fig. 2. Inhibition of SXA-catalyzed hydrolysis of 4NPX by L-arabinose and D-ribose at 25 °C. (a) L-Arabinose. SXA was preincubated for 1 h at 25 °C in constant ionic strength buffer ($I = 0.3$ M) containing varied concentrations of L-arabinose: 100 mM succinate-NaOH at pH 5.0 (■), 100 mM sodium phosphate at pH 7.0 (▲), and 30 mm sodium pyrophosphate at pH 9.0 (●). For determination of initial rates, an aliquot (7 μL) of preincubated enzyme was added to 1-mL reaction mixtures at 25 °C containing 4NPX concentrations at $<0.2 \times K_m$ in the same buffer and same L-arabinose concentration as the preincubation. Curves were generated by fitting initial-rate data to Eq. (3) treating substrate concentrations and previously determined K_m(4NPX) values as constants: at pH 5.0, K_i(L-arabinose) = 49.5 ± 1.8 mM, K_{i2}(L-arabinose) = 34.9 ± 2.4 mM, k_{cat} = 22.6 ± 0.1 s^{-1}, K_m(4NPX) = 0.895 ± 0.028 mM, [4NPX] = 0.10 mM; at pH 7.0, K_i(L-arabinose) = 20.4 ± 1.5 mM, K_{i2}(L-arabinose) = 111 ± 29 mM, k_{cat} = 11.4 ± 0.1 s^{-1}, K_m(4NPX) = 0.38 ± 0.01 mM, [4NPX] = 0.05 mM; at pH 9.0, K_i(L-arabinose) = 14.2 ± 0.3 mM, K_{i2} (L-arabinose) = 10^{18} mM, k_{cat} = 0.545 ± 0.004 s^{-1}, K_m(4NPX) = 0.315 ± 0.011 mM, [4NPX] = 0.05 mM. Note that the right ordinate scale, for pH's 5 and 7, is expanded 4-fold in comparison to the left ordinate scale for pH 9. (b) D-Ribose. For determination of initial rates, an aliquot (7 μL) of SXA (in 10 mM sodium phosphate, pH 7.0) was added to 1-mL reaction mixtures at 25 °C containing 4NPX at $<0.2 \times K_m$, varied concentrations of D-ribose and constant ionic strength buffers ($I = 0.3$ M): 100 mM succinate-NaOH at pH 5.0 (□), 100 mM sodium phosphate at pH 7.0 (Δ), and 30 mm sodium pyrophosphate at pH 9.0 (○). Curves were generated by fitting initial-rate data to Eq. (3) treating substrate concentrations and previously determined K_m(4NPX) values as constants: at pH 5.0, K_i(D-ribose) = 18.0 ± 1.0 mM, K_{i2}(D-ribose) = 81.2 ± 14.3 mM, k_{cat} = 25.9 ± 0.1 s^{-1}, K_m(4NPX) = 0.895 ± 0.028 mM, [4NPX] = 0.10 mM; at pH 7.0, K_i(D-ribose) = 11.9 ± 0.2 mM, K_{i2} (D-ribose) = 107 ± 6 mM, k_{cat} = 12.1 ± 0.02 s^{-1}, K_m(4NPX) = 0.38 ± 0.01 mM, [4NPX] = 0.05 mM; at pH 9.0, K_i(D-ribose) = 14.8 ± 0.7 mM, K_{i2}(D-ribose) = 5730 ± 22000 mM, k_{cat} = 0.369 ± 0.004 s^{-1}, K_m(4NPX) = 0.315 ± 0.012 mM, [4NPX] = 0.05 mM. Note that the right ordinate scale, for pHs 5 and 7, is expanded 6-fold in comparison to the left ordinate scale for pH 9.

noncompetitive with respect to substrate 4NPX: the data fit to Eq. (2) better than to Eq. (1) according to the low F test probabilities (0.00% and 0.13% for experiments 2a and 2b, respectively) that the data fit the two equations equally well, even though the K_{is} values determined from fitting the data to Eq. (2) are greater than 100-fold the determined value for K_m(4NPX) of 0.38 mM and it is difficult to distinguish between competitive and noncompetitive inhibition by visual inspection of the $1/v$ versus 1/4NPX plot (Figure S1A of Supplementary data). Experimental distinction between competitive and noncompetitive inhibition is more difficult when the ratio $K_i * K_{is}/K_m$ of Eq. (2) is high relative to K_i; therefore, experimental determination of noncompetitive inhibition is more difficult when the ratio K_{is}/K_m is high. In comparison to K_i values (3.79 and 3.82 mM) from fitting the pH 7.0 data of experiments 2a and 2b for D-xylose inhibition of 4NPX hydrolysis to Eq. (1), the K_i values (4.16 and 4.04 mM) from fitting the same data to Eq. (2) are closer to the K_i values (4.27 and 4.42 mM) determined at pH 7.0 for D-xylose inhibition of 4NPA hydrolysis by fitting the data of experiments 3a and 3b to Eq. (1) (Table 1). Clearly, K_i values (dissociation constant for I from EI) for inhibition by D-xylose should be independent of substrate, unless factor(s) unaccounted for by the equation contribute to the inhibition [i.e., the $K_m * I/K_i * K_{is}$ term of Eq. (2)]. Noncompetitive inhibition of SXA-catalyzed 4NPX hydrolysis by D-xylose is stronger at pH 5.3. For three data sets collected at pH 5.3 with 4NPX as substrate, F tests indicate 0.00% probability that the data fit Eq. (1) as well as Eq. (2) and the ratios of K_{is}/K_m from Eq. (2) are between 16 and 23, showing that the EIS complex of SXA, D-xylose and 4NPX is more populated at pH 5.3 than at pH 7.0. In addition, noncompetitive inhibition is more clearly evident by visual inspection of the $1/v$ versus 1/4NPX plot of pH 5.3 data (Figure S1B of Supplementary data). Furthermore, differences between K_i(D-xylose) values determined by using Eq. (1) and (2) are larger with the data obtained at pH 5.3: in three experiments with 4NPX as substrate, K_i(D-xylose) = 9.41 ± 0.44, 10.6 ± 0.5 and 9.04 ± 0.31 mM from fitting data to Eq. (2) and K_i(D-xylose) = 7.38 ± 0.27, 8.58 ± 0.37 and 7.62 ± 0.26 mM from fitting the same data to Eq. (1); with 4NPA as substrate, K_i(D-xylose) = 11.6 ± 0.5 mM from fitting data to Eq. (1) or Eq. (2) (Table S2 of Supplementary data). At pH 5.3 with 4NPA as substrate, D-xylose remains a competitive inhibitor with respect to substrate: F test indicates 99.95% probability that the data fit Eq. (1) as well as Eq. (2) and the determined value for K_{is} is enormous (10^{16} M) (Table S2 of Supplementary data). Therefore, D-xylose is a competitive inhibitor with respect to substrate 4NPA (forms only an EI complex) and it is a noncompetitive inhibitor with respect to substrate 4NPX (forms EI and EIS complexes).

At pH 7.0, inhibition by L-xylose appears noncompetitive with respect to substrate 4NPA: F test probabilities for the two determinations (experiments 3a and 3b) are 0.03% and 7.9% that the data fit Eq. (1) as well as Eq.

(2); K_{is} values of 43.5 ± 9.3 mM and 64.7 ± 36.3 mM with K_{is}/K_m ratios of 40.3 and 59.9 and K_{is}/K_i ratios of 3.1 and 5.0 were determined from Eq. (2) (Table 1). Noncompetitive inhibition with respect to substrate 4NPA by L-xylose is better established by data obtained at pH 5.3: the F test probability, from a single experiment, is 0.00% that the data fit Eq. (1) as well as Eq. (2) and the K_{is} value of 5.83 ± 1.17 mM, the K_{is}/K_m ratio of 5.40, and the K_{is}/K_i ratio of 0.14 were determined from Eq. (2) (Table S2 of Supplementary data). At pH 7.0, noncompetitive inhibition with respect to substrate 4NPX by L-xylose appears less certain: F test probabilities for the two determinations (experiments 2a and 2b, Table 1) are 37.7% and 21.9% that the data fit Eq. (1) as well as Eq. (2) and K_{is} values of 166 ± 189 mM and 121 ± 98 mM were determined from Eq. (2) with ratios of K_{is}/K_m of 437 and 318 and K_{is}/K_i ratios of 12.4 and 7.5 (Table 1). As with substrate 4NPA, noncompetitive inhibition by L-xylose with respect to substrate 4NPX is stronger at pH 5.3: the F test probability from a single experiment is 0.04% that the data fit Eq. (1) as well as Eq. (2) and the K_{is} value of 18.0 ± 5.11 mM, the K_{is}/K_m ratio of 23.3, and the K_{is}/K_i ratio of 0.53 were determined from Eq. (2) (Table S2 of Supplementary data). Therefore, L-xylose is a noncompetitive inhibitor with respect to substrates 4NPA and 4NPX (forms EI and EIS complexes with both substrates).

Double binding inhibitors

This group includes D-arabinose, L-arabinose, D-erythrose, and D-ribose. Each of these inhibitor data sets was further evaluated by fitting the data to Eq. (3) (double binding) and Eq. (5) (triple binding) and executing F test comparisons; in all cases the probability that the data fit Eq. (3) as well as Eq. (5) was high (91% for L-arabinose [$n = 11$], 88% for D-ribose [$n = 8$], 100% for D-arabinose [$n = 6$], and 100% for D-erythrose [$n = 2$]) and K_{i3} values were huge, indicating the lack of significance of the term for binding a third equivalent of inhibitor. Further examination of binding modes is from data obtained by varying substrate and inhibitor concentrations, fitting the data to Eqs. (3) and (4) for double binding with competitive or noncompetitive inhibition, respectively, and executing F tests for comparisons (Table 1). For D-ribose and D-arabinose, determined values for K_{is} from fitting data to Eq. (4) are huge in comparison to the K_m values and F test probabilities indicate that the data for inhibition of SXA-catalyzed hydrolysis of 4NPA and 4NPX fit Eq. (3) as well as Eq. (4). Therefore, these two double binding monosaccharides are competitive with respect to substrates 4NPA and 4NPX; they form EI and EII complexes but not EIS complexes (Scheme 1).

In the case of L-arabinose, data from experiments 2 and 3, fitted to Eqs. (3) and (4), indicate noncompetitive inhibition of 4NPX and 4NPA reactions: F tests for both substrates are 0.00% that the data fit Eq. (3) as well as Eq. (4) and K_{is}/K_m ratios are 9.1 with substrate 4NPX and 4.7 with substrate 4NPA (Table 1). In the case of D-erythrose, data from experiment 2 of Table 1 indicates noncompetitive inhibition of the 4NPX reaction: F test probability is 0.00% that the data fit Eq. (3) as well as Eq. (4) and the K_{is}/K_m ratio is 32.9. Data from experiment 3 indicates noncompetitive inhibition by D-erythrose with respect to substrate 4NPA: F test probability is 1.2% that

Fig. 3. Slow binding of L-arabinose to SXA. Enzyme was preincubated in the presence (···) or absence (—) of 300 mM L-arabinose in 100 mM sodium phosphate, $I = 0.3$ M, pH 7.0, for a minimum of 10 min at 4 °C followed by ~3 min at 25 °C. (a) Burst. Aliquots (7.0 μL) of preincubated enzyme (38.6 μM monomer) were added to the 1-mL reaction mixtures containing 1.0 mM 4NPX and 300 mM L-arabinose in 100 mM sodium phosphate, $I = 0.3$ M, pH 7.0, at 25 °C. Absorbance at 400 nm of reaction progress was recorded for 3 min. The 12 s delay for starting data acquisition was due to the time needed for enzyme addition and mixing. Absorbance data of the reaction with enzyme preincubated in the absence of L-arabinose (—) were fitted to Eq. (12): $v_s = (1.02 \pm 0.0002) \times 10^{-3}$ AU s^{-1}, $v_0 = (2.55 \pm 0.02) \times 10^{-3}$ AU s^{-1}, $k_{obs} = 0.0589 \pm 0.0003$ s^{-1}. Absorbance data of the reaction with enzyme preincubated in the presence of 300 mM L-arabinose (···) were fitted to the steady-state portion of Eq. (12) (Absorbance $= d + v_s * t$): $v_s = (1.04 \pm 0.0002) \times 10^{-3}$ AU s^{-1}. (b) Lag. Aliquots (7.0 μL) of preincubated enzyme (7.7 μM) were added to reaction mixtures containing 1.0 mM 4NPX and 100 mM sodium phosphate, $I = 0.3$ M, pH 7.0 at 25 °C. Absorbance at 400 nm was recorded for 3 min. The 12 s delay for starting data acquisition was due to mixing. Absorbance data of the enzyme reaction with enzyme preincubated in the absence of L-arabinose (—) were fitted to the steady-state portion of Eq. (12) (Absorbance $= d + v_s * t$): $v_s = (4.81 \pm 0.001) \times 10^{-3}$ AU s^{-1}. Absorbance data of the enzyme reaction with enzyme preincubated in the presence of 300 mM L-arabinose (···) were fitted to Eq. (12): $v_s = (4.49 \pm 0.0005) \times 10^{-3}$ AU s^{-1}, $v_0 = (8.78 \pm 0.12) \times 10^{-4}$ AU s^{-1}, $k_{obs} = 0.0374 \pm 0.00009$ s^{-1}. (c) Representative burst data obtained using stopped-flow. Left syringe of stopped-flow contained 100 mM sodium phosphate, $I = 0.3$ M, pH 7.0 at 25 °C and the following concentrations of SXA in μM: 30.4 (Δ), 15.2 (■), 7.6 (□), 3.8 (●) and 1.9 (○). Right syringe contained 87 mM sodium phosphate, $I = 0.26$ M, pH 7.0 at 25 °C, 1.93 mM 4NPA and the following concentrations of L-arabinose in mM: 1500 (Δ), 750 (■), 375 (□), 187.5 (●), 93.8 (○). Reactions were monitored at 400 nm and the traces were normalized to final SXA concentration for presentation. Data were fitted to Eq. (12) for each trace with final L-arabinose concentrations in mM: 750 ($v_s = (8.00 \pm 0.01) \times 10^{-3}$ s^{-1}, $v_0 = (4.13 \pm 0.03) \times 10^{-2}$ s^{-1}, $k_{obs} = 0.151 \pm 0.0009$ s^{-1}), 375 ($v_s = (2.92 \pm 0.001) \times 10^{-2}$ s^{-1}, $v_0 = (9.74 \pm 0.04) \times 10^{-2}$ s^{-1}, $k_{obs} = 0.108 \pm 0.0006$ s^{-1}), 187.5 ($v_s = (9.16 \pm 0.005) \times 10^{-2}$ s^{-1}, $v_0 = 0.208 \pm 0.001$ s^{-1}, $k_{obs} = 0.0684 \pm 0.0003$ s^{-1}), 93.8 ($v_s = 0.235 \pm 0.0001$ s^{-1}, $v_0 = 0.379 \pm 0.001$ s^{-1}, $k_{obs} = 0.0350 \pm 0.0003$ s^{-1}), 46.9 ($v_s = 0.481 \pm 0.0002$ s^{-1}, $v_0 = 0.645 \pm 0.001$ s^{-1}, $k_{obs} = 0.0243 \pm 0.0002$ s^{-1}), and $v_s = 1.42$ s^{-1} for SXA in the absence of L-arabinose. (d) Dixon plots of $1/v_0$ and $1/v_s$ versus [L-arabinose]. Values of v_0 and v_s at varied [L-arabinose] were obtained from stopped-flow experiments described in (c), and fitted to Eq. (4) with constant values for $S = 0.965$ mM 4NPA, K_m(4NPA) = 1.08 mM, and K_{is}(4NPA) = 5.07 mM: for $1/v_0$ versus [L-arabinose], $K_i = 24.0 \pm 0.3$ mM and $K_{i2} = 620 \pm 53$ mM; for $1/v_s$ versus [L-arabinose], $K_i = 19.8 \pm 0.1$ mM and $K_{i2} = 99.2 \pm 1.7$ mM. (e) Dependence of k_{obs} on the concentration of L-arabinose at (○) 0.965 mM 4NPA and (●) 4.2 mM 4NPA. To obtain the fitted curves, values of k_{obs} at varied [L-arabinose] and [4NPA] were fitted globally to Eq. (13) with constant values for K_m(4NPA) = 1.08 mM, $K_i = 20.3$ mM (from Table 1, experiment 3), and $K_{is} = 5.07$ mM (from Table 1, experiment 3): $k_{off} = 0.0213 \pm 0.0064$ s^{-1}, $k_{on} = 0.203 \pm 0.011$ s^{-1}, and $K_{i2(rapid)} = 314 \pm 63$ mM. Upper curve, 0.965 mM 4NPA; lower curve, 4.2 mM 4NPA.

the data fit Eq. (3) as well as Eq. (4) and the K_{is}/K_m ratio is 109. Therefore, inhibitors L-arabinose and D-erythrose form EI, EII, and EIS complexes, and EIS can form with either 4NPA or 4NPX.

Slow binding L-arabinose

Unlike the other inhibitors of SXA described in this work, in experiments conducted to determine equilibrium inhibition constants for L-arabinose, it was necessary to preincubate SXA in reaction mixtures containing L-arabinose but lacking substrate prior to initiating complete reactions by adding an aliquot of the preincubation mixture to reaction mixtures containing substrate and the same concentration of L-arabinose as in the preincubation. The preincubation step was necessary because inhibition of SXA catalysis by L-arabinose shows time dependence on the order of minutes (Fig. 3a). When SXA, preincubated (10 min at 4 °C followed by ~3 min at 25 °C) at pH 7.0 in the absence of L-arabinose, was added to the reaction mixture containing 300 mM L-arabinose and 1 mM 4NPX at pH 7.0 and 25 °C, there was a noticeable burst ($v_0 = 2.55 \times 10^{-3}$ AU s^{-1}) in 4NPX hydrolysis activity reported by the 400 nm absorbance. Reaction progress equilibrated within a few minutes to a steady-state rate ($v_s = 1.02 \times 10^{-3}$ AU s^{-1}), which matches the steady-state rate ($v_s = 1.04 \times 10^{-3}$ AU s^{-1}) of a similar reaction (300 mM L-arabinose and 1 mM 4NPX at pH 7.0 and 25 °C) that was initiated by SXA preincubated (10 min at 4 °C followed by ~3 min at 25 °C) in the presence of 300 mM L-arabinose at pH 7.0; the latter reaction exhibited neither a burst nor lag of 4NPX hydrolysis activity. The reaction progress data were fitted to Eq. (12) for determinations of v_0 and v_s [19,20]. Notably, for the reaction

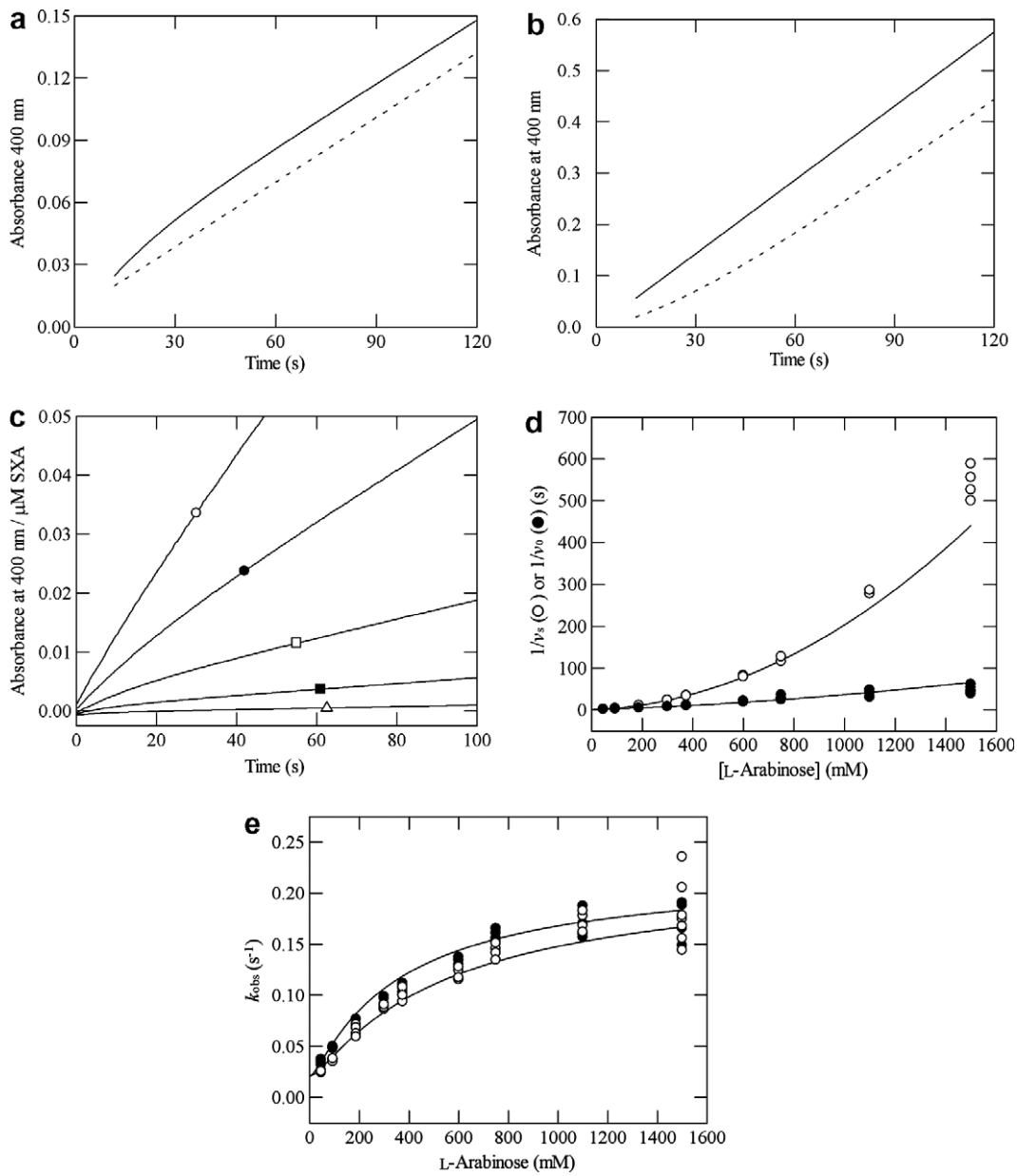

initiated with SXA preincubated in the absence of 300 mM L-arabinose, the 4NPX hydrolysis reaction rate was inhibited by 90% in the rapid phase and by an additional 6% in the slow phase for a combined effect of 96% inhibition in the steady state in comparison to the uninhibited rate from a similar reaction in the absence of L-arabinose.

Reversibility of L-arabinose inhibition is demonstrated by reactions containing 1 mM 4NPX initiated by adding a small aliquot of SXA preincubated in the absence or presence of 300 mM L-arabinose (Fig. 3b). Progress of the 4NPX hydrolysis reaction initiated by SXA preincubated in the presence of 300 mM L-arabinose shows a lag in rate initially ($v_0 = 8.78 \times 10^{-4}$ AU s^{-1}) that equilibrates within minutes to a steady-state rate ($v_s = 4.49 \times 10^{-3}$ AU s^{-1}), which is 93% that of the steady-state rate ($v_s = 4.81 \times 10^{-3}$ AU s^{-1}) estimated for a similar reaction initiated with SXA preincubated in the absence of L-arabinose; the latter reaction exhibited neither a burst nor lag of 4NPX hydrolysis. The 7% difference between the two steady-state rates is mainly attributable to the small carry-over of L-arabinose (2.1 mM final in the reaction) with the aliquot of SXA used to initiate the reaction. From fitting data for the reaction progression initiated with SXA preincubated in 300 mM L-arabinose to Eq. (12), a k_{obs} value of 0.0374 s^{-1} at 1 mM 4NPX was determined. The k_{obs} value from this dilution experiment is the off rate (k_{off}) for L-arabinose from SXA in the slow phase. For SXA preincubated in the presence of 300 mM L-arabinose at pH 7.0 and 25 °C followed by 1000-fold dilution into reaction mixtures at pH 7.0 and 25 °C and the indicated substrate concentrations, the following k_{off} values were determined by fitting data from the hydrolysis reaction progressions to Eq. (12): 0.26 mM 4NPA ($k_{off} = 0.0401 \pm 0.0003$ s^{-1}), 1.02 mM 4NPA ($k_{off} = 0.0359 \pm 0.001$ s^{-1}), 7.67 mM 4NPA ($k_{off} = 0.0357 \pm 0.0002$ s^{-1}), 0.3 mM 4NPX ($k_{off} = 0.0394 \pm 0.0003$ s^{-1}), and 7.5 mM 4NPX ($k_{off} = 0.0329 \pm 0.0003$ s^{-1}) for a mean k_{off} value of 0.0368 ± 0.0030 s^{-1}; for reference, K_m(4NPA) = 1.08 mM and K_m(4NPX) = 0.38 mM at pH 7.0 and 25 °C. Thus, k_{off} is independent of the substrate concentration at pH 7.0 and 25 °C.

Stopped-flow data recording absorbance changes at 400 nm were collected from several reactions that were initiated by mixing 50 μl of SXA at pH 7.0 and 25 °C in one syringe with 50 μl of varied concentrations of L-arabinose and 1.93 or 8.40 mM 4NPA at pH 7.0 and 25 °C in the other syringe (Fig. 3c). The data were fitted to Eq. (12) for determination of v_0, v_s and k_{obs} values for the rapid and slow inhibition phases. Dixon plots of Fig. 3d show that, for reactions at 0.965 mM 4NPA, the $1/v_s$ versus [L-arabinose] curve is concave upward similar to the Dixon plot ($1/v$ versus [L-arabinose]) of Fig. 2a at pH 7.0, whereas the $1/v_0$ versus [L-arabinose] curve is nearly linear. Similar Dixon plot curves are produced from the data acquired at 4.2 mM 4NPA (Figure S2 of Supplementary data). Fitting the Dixon plot values of Fig. 3d (0.965 mM 4NPA) to Eq. (3) provides K_i(L-arabinose) = 19.8 mM and K_{i2}(L-arabinose) = 99.2 mM for $1/v_s$ versus [L-arabinose] and K_i(L-arabinose) = 24.0 mM and K_{i2}(L-arabinose) = 620 mM for $1/v_0$ versus [L-arabinose]. Similarly, fitting the Dixon plot values of Figure S2 (4.2 mM 4NPA) to Eq. (3) provides K_i(L-arabinose) = 19.8 mM and K_{i2}(L-arabinose) = 93.8 mM for $1/v_s$ versus [L-arabinose] and K_i(L-arabinose) = 37.4 mM and K_{i2}(L-arabinose) = 389 mM for $1/v_0$ versus [L-arabinose]. Thus, there is an initial rapid binding event for binding the second equivalent of L-arabinose followed by a slow-binding phase where affinity is increased 5-fold as represented by the relationships of Scheme 2. The value for k_{on} can be calculated from the equilibrium values for K_{i2}(L-arabinose) from the $1/v_s$ versus [L-arabinose] Dixon plots, the values for $K_{i2(rapid)}$(L-arabinose) from the $1/v_0$ versus [L-arabinose] Dixon plots, and the value for k_{off} (0.0368 ± 0.0030 s^{-1}) from the dilution experiments by using the relationship $K_{i2} = K_{i2(rapid)}/(1 + k_{on}/k_{off})$: from the 0.965 mM 4NPA data, $k_{on} = 0.193 \pm 0.025$ s^{-1}; and from the 4.2 mM 4NPA data, $k_{on} = 0.116 \pm 0.015$ s^{-1}.

More direct methods for determination of k_{on} values rely on k_{obs} values from the stopped-flow experiments. k_{obs} values from the 0.965 and the 4.2 mM 4NPA stopped-flow experiments are similar at each L-arabinose concentration (Fig. 3e), indicating that there is little influence of the 4NPA concentration on the observed rate constant under these conditions. The curves of Fig. 3e represent global fitting the k_{obs} values of the combined experiments (0.965 and 4.2 mM 4NPA) to Eq. (13), which reflects a classical binding equation that defines k_{on} as saturable and dependent on the fraction of enzyme in the rapidly established EII form with determined values of $k_{on} = 0.203$ s^{-1}, $k_{off} = 0.0213$ s^{-1}, and $K_{i2(rapid)} = 314$ mM. Data scatter in the k_{obs} versus [L-arabinose] plot of Fig. 3e and the low estimate for k_{off} might be expected given that, in the determinations of k_{off} and k_{on} rates from burst experiments, there is always a larger population of EI in comparison to that of EII and EII* and uninhibited enzyme activity is the reporter. The lag experiments more accurately determined k_{off} because, upon dilution, EII and EI can rapidly dissipate to $E + I$, leaving EII* as the only inhibited complex. Better determinations of k_{on} and k_{off} rates from the burst experiments would require means to kinetically isolate EI from EII and EII*.

Influence of pH on inhibitor binding

pH dependencies of inhibition constants were determined for D-glucose, D-xylose, D-ribose, and L-arabinose in buffers of constant ionic strength and 25 °C. The studies were limited to pH values of 4.3 and above (to pH 10) due to the instability of SXA at lower pH [3,4]. SXA retains full catalytic activity following 1 h incubation at 25 °C and between pH 4.3 and 10 [4]. Inhibition data for D-xylose were obtained by varying 4NPX and inhibitor concentrations at each pH and fitting the data to Eq. (2) for noncompetitive inhibition. Determined values for $1/K_i$ and $1/K_{is}$

are plotted in Fig. 4. The $1/K_i$ plot indicates two protonatable groups [pK_as 5.08 and 6.75 from fitting the values to Eq. (17)] corresponding to the two acidic limbs (Fig. 4a). Fitting the $1/K_i$ values to Eq. (17) (two protonatable groups) is preferred over that of Eq. (14) (single protonatable group) from inspection and from the F test analysis (Fig. 4a legend). In terms of Fig. 1, the limit of $1/K_i = 0.152\ \mathrm{mM}^{-1}$ (associated with pK_a 5.08) reflects binding to the D14$^-$E186^H form of SXA and the limit $1/K_i = 0.284\ \mathrm{mM}^{-1}$ (associated with pK_a 6.75) reflects binding to the D14$^-$E186$^-$ form; the ratio of the two limits indicates that D-xylose binds to D14$^-$E186$^-$ SXA with 0.9-fold greater affinity than to D14$^-$E186^H SXA. The $1/K_i$(D-xylose) pH profile resembles the pH dependency of $1/K_m$(4NPX) for SXA where 4NPX has 0.9-fold greater affinity for the catalytically inactive enzyme form (D14$^-$E186$^-$) than the catalytically active enzyme form (D14$^-$E186^H) [3]. Determined $1/K_{is}$(D-xylose) values have a bell-shaped pH dependency [pK_as 4.75 and 6.64 from fitting the $1/K_{is}$ (D-xylose) values to Eq. (16)] (Fig. 4b), indicating that formation of EIS occurs only with the catalytically active form of SXA (D14$^-$E186^H) and EIS does not form with the catalytically inactive forms of SXA (D14^{H}E186^H and D14$^-$E186$^-$).

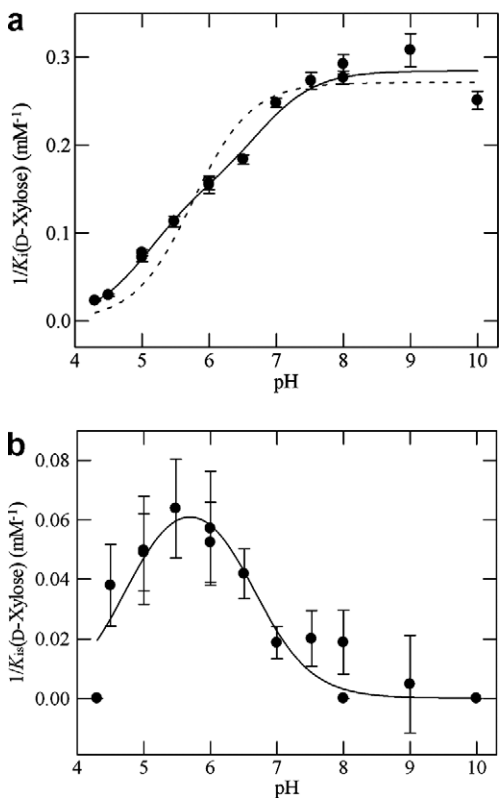

Fig. 4. Influence of pH on inhibition of SXA-catalyzed hydrolysis of 4NPX by D-xylose. Initial rates were determined from reactions containing varied concentrations of 4NPX and D-xylose. Initial-rate data ($n = 30$) were fitted to Eq. (2) to determine K_i and K_{is} values at each pH; standard errors are indicated. (a) The solid curve was generated by fitting $1/K_i$ values at each pH to Eq. (17) (two protonatable groups): limit 1 of $1/K_i$(D-xylose) $= 0.152 \pm 0.020\ \mathrm{mM}^{-1}$, limit 2 of $1/K_i$(D-xylose) $= 0.284 \pm 0.011\ \mathrm{mM}^{-1}$, p$K_{a1} = 5.08 \pm 0.07$, p$K_{a2} = 6.75 \pm 0.27$, and reduced $\chi^2 = 0.00224$. The dotted curve was generated by fitting K_i(D-xylose) values at each pH to Eq. (14) (single protonatable group): pH-independent $1/K_i$(D-xylose) $= 0.271 \pm 0.011\ \mathrm{mM}^{-1}$, p$K_a = 5.76 \pm 0.11$, and reduced $\chi^2 = 0.00843$. F test indicates that there is a 0.65% probability that the data fit Eq. (14) as well as Eq. (17). (b) The solid curve was generated by fitting $1/K_{is}$ values at each pH to Eq. (16): pH-independent $1/K_{is}$ (D-xylose) $= 0.0748 \pm 0.0127\ \mathrm{mM}^{-1}$, p$K_{a1} = 4.75 \pm 0.22$, and p$K_{a2} = 6.64 \pm 0.25$.

Inhibition data for D-glucose was obtained as for D-xylose, but the data were fitted to Eq. (1) describing competitive inhibition. Similar to D-xylose and 4NPX, the $1/K_i$ plot for D-glucose inhibition of 4NPX hydrolysis shows two acidic limbs with pK_as 5.07 and 7.39 determined by fitting the $1/K_i$ values to Eq. (17) (Fig. 5). The limit ($1/K_i$ (D-glucose) $= 0.0566\ \mathrm{mM}^{-1}$) associated with p$K_a$ 7.39 and the limit ($1/K_i$(D-glucose) $= 0.0193\ \mathrm{mM}^{-1}$) associated with p$K_a$ 5.07 indicate that D-glucose binds to D14$^-$E186$^-$ SXA with 1.9-fold greater affinity than to D14$^-$E186^H SXA. EI does not form with D14^{H}E186^H [implicit in Eq. (17)].

For inhibitors, L-arabinose and D-ribose, which can bind twice to SXA forming EI and EII complexes, the pH dependence of inhibition parameters ($1/K_i$ and $1/K_{i2}$) were determined from reactions that maintained low concentrations of 4NPX ($<0.2 \times K_m$). The low substrate concentrations avoid formation of EIS, which forms in the case of L-arabinose, and allow good determinations of K_i and K_{i2} by fitting the initial rate data to Eq. (3) with fixed values for K_m (determined at each pH) and substrate concentration. As for other equilibrium determinations with L-arabinose, SXA was preincubated in the same buffer and L-arabinose concentration of the reaction mixtures. The $1/K_i$ versus pH values were fitted to Eq. (17): for L-arabinose, the two acid limbs have p$K_{a1} = 4.69$ and p$K_{a2} = 7.24$ with respective limits of $1/K_i$(L-arabinose) $= 0.0275\ \mathrm{mM}^{-1}$ and $0.0660\ \mathrm{mM}^{-1}$ (Fig. 6a); for

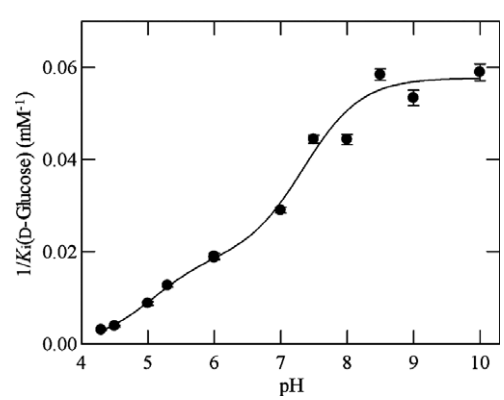

Fig. 5. Influence of pH on inhibition of SXA-catalyzed hydrolysis of 4NPX by D-glucose. Initial rates were determined from reactions containing varied concentrations of 4NPX and D-glucose. Initial-rate data ($n = 30$) were fitted to Eq. (1) to determine K_i values at each pH; standard errors are indicated. The curve was generated by fitting $1/K_i$ values at each pH to Eq. (17) (two protonatable groups): limit 1 of $1/K_i$ (D-Glucose) $= 0.0193 \pm 0.0015\ \mathrm{mM}^{-1}$, limit 2 of $1/K_i$(D-Glucose) $= 0.0566 \pm 0.0026\ \mathrm{mM}^{-1}$, p$K_{a1} = 5.07 \pm 0.05$, and p$K_{a2} = 7.39 \pm 0.14$.

D-ribose, the acidic and basic limbs are governed by pK_{a1} 4.91 and pK_{a2} 7.30, respectively, with respective limits of $1/K_i$(D-ribose) = 0.106 mM^{-1} and 0.0604 mM^{-1} (Fig. 7a). Thus, the first equivalent of L-arabinose binds D14$^-$E186$^-$ SXA with 1.4-fold greater affinity than D14$^-$E186^H SXA, and the first equivalent of D-ribose binds D14$^-$E186^H SXA with 0.75-fold greater affinity than D14$^-$E186$^-$ SXA.

Dixon plots for L-arabinose and D-ribose are curvilinear at pH 5 and pH 7, but they are linear at pH 9, suggesting two equivalents of inhibitor bind at the lower pH values

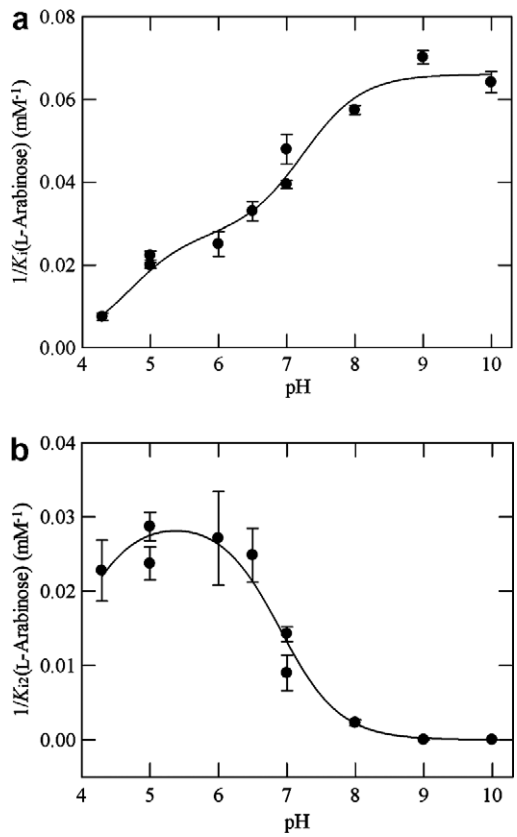

Fig. 6. Influence of pH on inhibition of SXA-catalyzed hydrolysis of 4NPX by L-arabinose. Enzyme was preincubated for at least 10 min at 4 °C followed by ~3 min at 25 °C in the same [L-arabinose] and same buffer (I = 0.3 M) as that in the individual reactions. Aliquots (7.0 μL) of preincubated enzyme were added to initiate reactions (1-mL at 25 °C) containing 4NPX at <0.2 × K_m(4NPX) in buffers of constant ionic strength (I = 0.3 M). Initial-rate data (n = 12) were fitted to Eq. (3) to determine K_i and K_{i2} values at each pH; standard errors are indicated. (a) The solid curve was generated by fitting $1/K_i$ values at each pH to Eq. (17) (two protonatable groups): limit 1 of $1/K_i$(L-arabinose) = 0.0275 ± 0.0037 mM^{-1}, limit 2 of $1/K_i$(L-arabinose) = 0.0660 ± 0.0054 mM^{-1}, pK_{a1} = 4.69 ± 0.12, pK_{a2} = 7.24 ± 0.26, and reduced χ^2 = 0.0000960. When the data were fitted to Eq. (14) (single protonatable group), reduced χ^2 = 0.000994 (fitted curve is not shown). F test indicates that there is a 1.1% probability that the data fit Eq. (14) as well as Eq. (17). (b) $1/K_{i2}$ versus pH. The curve was generated by fitting $1/K_{i2}$ values at each pH to Eq. (16) (two protonatable groups): pH-independent $1/K_{i2}$(L-arabinose) = 0.0298 ± 0.0024 mM^{-1}, pK_{a1} = 3.85 ± 0.27, and pK_{a2} = 6.90 ± 0.13. Fitting $1/K_{i2}$ values at each pH to Eq. (15) (single protonatable group) provides the following: pH-independent $1/K_{i2}$(L-arabinose) = 0.0266 ± 0.0017 mM^{-1}, and pK_a = 7.02 ± 0.15. F test indicates 8.6% probability that the data fit Eq. (15) as well as Eq. (16).

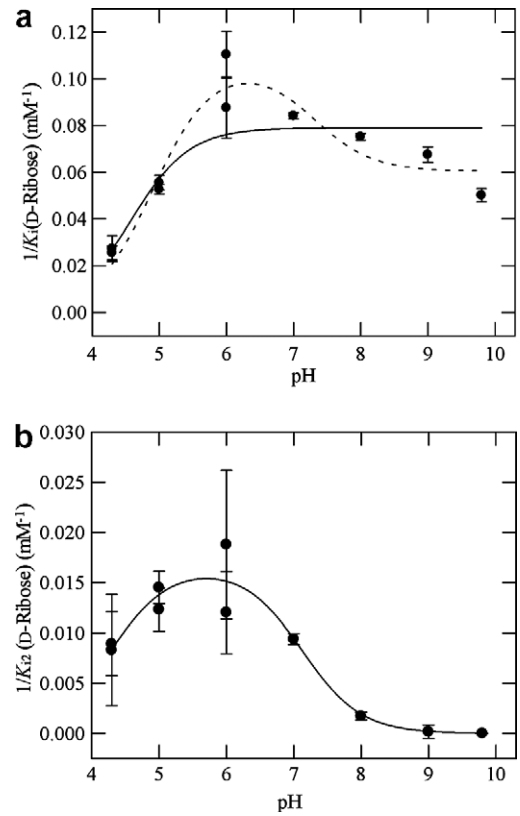

Fig. 7. Influence of pH on inhibition of SXA-catalyzed hydrolysis of 4NPX by D-ribose. Reactions (1-mL at 25 °C) contained varied concentrations of D-ribose and 4NPX at <0.2 × K_m. Initial-rate data (n = 12) were fitted to Eq. (3) to determine K_i and K_{i2} values at each pH; standard errors are indicated. (a) The solid curve was generated by fitting $1/K_i$ values at each pH to Eq. (14): pH-independent $1/K_i$ (D-ribose) = 0.0790 ± 0.0072 mM^{-1}, pK_a = 4.58 ± 0.25, the reduced χ^2 value = 0.0023. The dotted curve was generated by fitting $1/K_i$ values at each pH to Eq. (17): limit 1 of $1/K_i$(D-ribose) = 0.106 ± 0.012 mM^{-1}, limit 2 of $1/K_i$(D-ribose) = 0.0604 ± 0.0071 mM^{-1}, pK_{a1} = 4.91 ± 0.15, pK_{a2} = 7.30 ± 0.55, and reduced χ^2 value = 0.00062. F test indicates 2.7% probability that the data fit Eq. (14) as well as Eq. (17). (b) $1/K_{i2}$ versus pH. The curve was generated by fitting K_{i2} values at each pH to Eq. (16): pH-independent $1/K_{i2}$(D-ribose) = 0.0166 ± 0.0016 mM^{-1}, pK_{a1} = 4.29 ± 0.18 pK_{a2} = 7.12 ± 0.23. Fitting $1/K_{i2}$ values at each pH to Eq. (15) provides the following (curve not shown): pH-independent $1/K_{i2}$(D-ribose) = 0.0125 ± 0.0013 mM^{-1}, pK_a = 7.47 ± 0.45. F test indicates 0.64% probability that the data fit Eq. (15) as well as Eq. (16).

and only a single equivalent of inhibitor binds at the higher pH (Fig. 2). pH profiles for the $1/K_{i2}$ values of L-arabinose and D-ribose produce bell-shaped curves and the values were fitted to Eq. (16): for L-arabinose, the pH-independent limit of 0.0298 mM^{-1} has an acidic limb with pK_{a1} 3.85 (data set is limited to pH 4.3 and above, so the value is not well determined, but it is statistically significant according to the legend of Fig. 6b) and a basic limb with pK_{a2} 6.90 (Fig. 6b). For D-ribose, the pH-independent limit of 0.0166 mM^{-1} has an acidic limb with pK_{a1} 4.29 and a basic limb with pK_{a2} 7.12 (Fig. 7b). Perturbation of pK_{a1} values for $1/K_{i2}$ of L-arabinose and D-ribose to significantly below pK_a 5 for D14 resembles the k_{cat}(4NPA) and k_{cat}(4NPX) pH profiles [3]; the lower pK_a values for k_{cat} are matched

by increases in the values for K_m at low pH (in formation the productive $D14^{-}E186^{H}$ complex with substrate), and the lower pK_a values for $1/K_{i2}$ are matched by increased K_i values for L-arabinose and D-ribose at low pH (in formation of $D14^{-}E186^{H}$ complex with the first equivalent of inhibitor). Outward shifts of the pK_a values by a pH unit or more would not be unusual in such cases [21], because the pH equilibrium shifts are paid for by binding events that are independent of the determined parameter. Clearly, the second equivalent of L-arabinose and D-ribose binds to EI formed with $D14^{-}E186^{H}$; the second equivalent of the inhibitors does not bind to EI formed with $D14^{-}E186^{-}$. As indicated above, EI does not form with $D14^{H}E186^{H}$ so binding of a second equivalent of inhibitor to $D14^{H}E186^{H}$ is irrelevant.

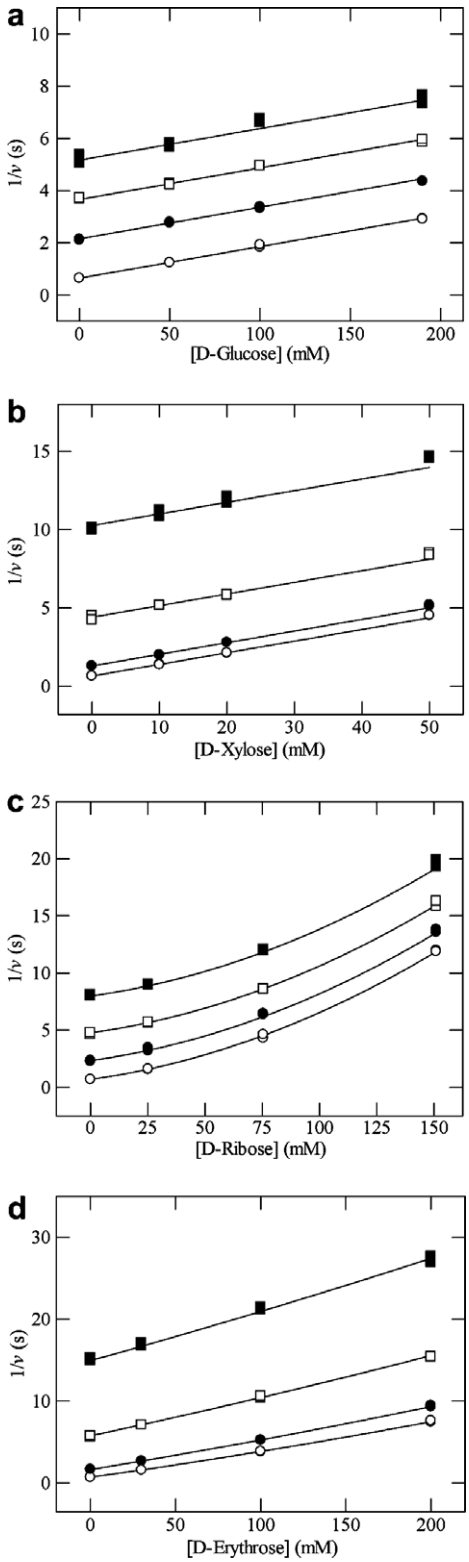

Fig. 8. Binding of mixed inhibitors to SXA. Reactions (1-mL) contained 100 mM sodium phosphate, $I = 0.3$ M, pH 7.0, 1.0 mM 4NPA, and varied concentrations of two different inhibitors at 25 °C. Reactions were initiated by adding an aliquot of SXA and monitored at 400 nm for 0.3 min. When L-arabinose was an inhibitor, SXA was preincubated in reaction mixture conditions, minus substrate, at room temperature (~25 °C) for at least 10 min; an aliquot of preincubated SXA was used to initiate the reactions. Dissociation constants determined from the initial rate data are listed in Table 2. (a) D-Glucose and D-xylose. D-Glucose concentrations are indicated; D-xylose concentrations are the following in mM: 0 (○), 20 (●), 40 (□), and 60 (■). The curve was generated by fitting the data to Eq. (6) with parameters shown in Table 2. (b) D-Xylose and D-ribose. D-Xylose concentrations are indicated; D-ribose concentrations are the following in mM: 0 (○), 20 (●), 80 (□), and 150 (■). The curve was generated by fitting the data to Eq. (8). (c) D-Ribose and L-arabinose. D-Ribose concentrations are indicated; L-arabinose concentrations are the following in mM: 0 (○), 50.4 (●), 101 (□), and 151 (■). The curve was generated by fitting the data to Eq. (11). (d) D-Erythrose and D-ribose. D-Erythrose concentrations are indicated; D-ribose concentrations are the following in mM: 0 (○), 30 (●), 100 (□), and 190 (■). The curve was generated by fitting the data to Eq. (11).

Inhibition of SXA catalysis by mixtures of two sugars at pH 7.0

Dixon plots of inhibition patterns when two competitive inhibitors are varied in reactions were used to decide whether pairs of inhibitors bind exclusively or nonexclusively to SXA (Fig. 8). In the classical case where both competitive inhibitors (I and X) bind singly to an active site, the $1/v$ versus [I] lines at fixed concentrations of inhibitor X lie parallel to one another when I and X are mutually exclusive and α of Scheme 1 is infinite; lines intersect to the left of the ordinate axis when the two inhibitors can bind simultaneously (nonexclusively) and α is finite. For SXA experiments, the concentration of substrate 4NPA was kept low at 1 mM ($<0.2 \times K_{is}$) to avoid significant formation of the EIS complex with L-arabinose and 4NPA. Among the six pairs of inhibitors examined for mixed inhibitor binding to SXA (Table 2), only one pair (D-glucose/D-xylose of Fig. 8a) exhibits the classical Dixon plot in which straight lines are produced when plotting $1/v$ versus [I] or [X]. Three inhibitor pairs (D-xylose/D-ribose of Fig. 8b, D-xylose/D-arabinose, and D-xylose/L-arabinose) can be plotted in linear form as $1/v$ versus [D-xylose] but not as $1/v$ versus [second inhibitor] because the second inhibitor binds twice (forming EI and EII complexes) and its Dixon plot is concave upward. The remaining two pairs

Table 2
Inhibition of SXA-catalyzed hydrolysis of 4NPA by mixtures of two sugars at pH 7.0 and 25 °C[a]

Exp. No.	Inhibitor I	K_i (mM)	K_{i2} (mM)	Inhibitor X	K_x (mM)	K_{x2} (mM)	α	*F* test probability (%)/ preferred equation	Binding mode[b]
1	D-Glucose	27.6 ± 0.2[c] 27.6 ± 0.2[d]		D-Xylose	4.42 ± 0.04[c] 4.43 ± 0.04[d]		 636 ± 1690[d]	71/Eq. (6)	E, SBI, SBX
2	D-Xylose	4.55 ± 0.04 [e] 4.57 ± 0.05[f]		D-Ribose	12.4 ± 0.3[e] 12.4 ± 0.3[f]	112 ± 8[e] 113 ± 8[f]	 183 ± 303[f]	55/Eq. (8)	E, SBI, DBX
3	D-Ribose	13.1 ± 0.4[g] 13.0 ± 0.4[h]	90.7 ± 8.0[g] 95.7 ± 8.5[h]	L-Arabinose	14.7 ± 0.6[g] 14.7 ± 0.6[h]	159 ± 20[g] 165 ± 20[h]	 36.1 ± 17.6[h]	4.9/Eq. (11)	NE, DBI, DBX
4	D-Arabinose	63.4 ± 2.7[e] 63.4 ± 2.7[f]	1110 ± 410[e] 1110 ± 420[f]	D-Xylose	4.26 ± 0.06[e] 4.25 ± 0.07[f]		 10^{17}[f]	100/Eq. (8)	E, DBI, SBX
5	D-Xylose	4.02 ± 0.07[e] 4.11 ± 0.07[f]		L-Arabinose	15.7 ± 1.1[e] 15.3 ± 0.9[f]	113 ± 20[e] 129 ± 21[f]	 31.1 ± 9.3[f]	0.17/Eq. (9)	NE, SBI, DBX
6	D-Erythrose	12.0 ± 0.3[g] 12.0 ± 0.1[h]	840 ± 210[g] 1260 ± 100[h]	D-Ribose	15.0 ± 0.6[g] 14.8 ± 0.1[h]	77.8 ± 8.0[g] 88.7 ± 2.0[h]	 13.2 ± 0.6[h]	0.00/Eq. (11)	NE, DBI, DBX

Significance of the α term was evaluated by fitting data from the same Exp. No. to the indicated two equations containing [Eqs. (7), (9), and (11)] or lacking [Eqs. (6), (8), and (10)] the α term and subjecting the two fittings to an *F* test; in all cases reported here, the % probability refers to the probability that the data fit the equation lacking the α term as well as the equation containing the term—the preferred equation is indicated.

[a] SXA competitive inhibition constants were determined from reactions containing 100 mM sodium phosphate, $I = 0.3$ M, pH 7.0, 1 mM 4NPA, varying concentrations of inhibitor I and inhibitor X at 25 °C. When L-arabinose was an inhibitor, SXA was preincubated in complete reaction mixture minus substrate at room temperature (~25 °C) for at least 10 min prior to addition to reaction mixtures.

[b] Conclusions based on preferred equation: E, exclusive binding (forms EI and EX); NE, nonexclusive binding (forms EI, EX, and EIX); SBI, single binding I (forms EI); DBI, double binding I (forms EI and EII); SBX, single binding X; DBX, double binding X.

[c] Initial-rate data were fitted to Eq. (6) with K_m(4NPA) = 1.08 mM set as a constant.

[d] Initial-rate data were fitted to Eq. (7) with K_m(4NPA) = 1.08 mM set as a constant.

[e] Initial-rate data were fitted to Eq. (8) with K_m(4NPA) = 1.08 mM set as a constant.

[f] Initial-rate data were fitted to Eq. (9) with K_m(4NPA) = 1.08 mM set as a constant.

[g] Initial-rate data were fitted to Eq. (10) with K_m(4NPA) = 1.08 mM set as a constant.

[h] Initial-rate data were fitted to Eq. (11) with K_m(4NPA) = 1.08 mM set as a constant.

(D-ribose/L-arabinose and D-erythrose/L-arabinose) comprise inhibitors, each of which binds twice so the Dixon plots are concave upward regardless of which inhibitor is varied in the plot (Figs. 8c and d) To evaluate the significance of α for mixed inhibitor binding, *F* tests compare fitting the data to equations that contain or lack the α term: for two single binding inhibitors, Eq. (6) (no α term) versus Eq. (7) (with α term); for one inhibitor binding once and the other inhibitor binding twice, Eq. (8) (no α term) versus Eq. (9) (with α term); and for two double binding inhibitors, Eq. (10) (no α term) versus Eq. (11) (with α term). The *F* test evaluations indicate that three of the inhibitor pairs can bind simultaneously:D-ribose/L-arabinose ($\alpha = 36.1$); D-xylose/L-arabinose ($\alpha = 31.1$); and D-erythrose/D-ribose ($\alpha = 13.2$) (Table 2). Among the other three pairs, D-arabinose and D-xylose cannot bind simultaneously, and it is unlikely that simultaneous binding occurs with the D-glucose/D-xylose pair or the D-xylose/D-ribose pair, given the data in Table 2. Thus, in the two cases where two double binding inhibitors were mixed (D-ribose/L-arabinose and D-erythrose/D-ribose), both pairs allowed simultaneous binding of the two inhibitors to form EIX. The other pair that can bind simultaneously (D-xylose and L-arabinose) comprise a single binding and a double binding inhibitor.

Summary and conclusion

An underlying property in the numerous inhibition constants determined for this work, is that none of the commonly occurring sugars of the survey bind with great affinity to SXA; the K_i values among 9 of the more potent inhibitors are mM in scale and vary in potency by less than 20-fold (4–67 mM). Acceptance of a broad range of inhibitors by the SXA active site contrasts with its rather narrow substrate acceptance: of 15 commercially available 4-nitrophenyl glycosides tested, only 4NPA and 4NPX serve as substrates for SXA [3]. Low affinities for inhibitors and substrates contrast with the numerous hydrogen bonds shared between active-site residues and substrate 1,4-β-D-xylobiose ($K_m = 2$ mM) [12]. Assuming the non-catalyzed rate of hydrolysis for xylobiose is similar to that of α-methylglucopyranoside [22], it has been estimated that SXA enhances the rate of xylobiose hydrolysis by a factor of 10^{17} and the dissociation constant for the transition state ($ES^{\ddagger}$) is $\sim 10^{-19}$ M [3]. Thus, binding selectivity and affinity for ground state ligands appear to have been largely sacrificed to catalysis in SXA. Although discovery of potent inhibitors of SXA is outside the scope of this study, it should be noted that 4-methylumbelliferyl-β-D-ribopyranoside constitutes the best example of a strong inhibitor of the homologous (62% identical protein sequence with SXA) β-xylosidase from *B. pumilus* having a K_i of 0.6 μM [23], and it has been suggested that the C2 hydroxyl group of the ribopyranoside may displace the active-site water molecule (water of hydrolysis) and mimic the transition state [18].

Extension of pH profiles from the substrate kinetic parameters to binding of active-site inhibitors (D-xylose, D-glucose, L-arabinose, and D-ribose) has served to substantiate the model of Fig. 1. In aqueous solution, the four monosaccharides and the sugars of Table 1 are predominantly pyranoses with D-ribose having the highest furanose content (20%) and aldehyde content (0.05%) [24]. All four of the inhibitory monosaccharides bind to $D14^{-}E186^{H}$ SXA: similar to the pH profile of $1/K_m$(4NPX), three of them bind better to the $D14^{-}E186^{-}$ SXA than to the $D14^{-}E186^{H}$ form; only D-ribose has the opposite preference. None of the four inhibitors mimics 4NPA by binding only to $D14^{-}E186^{H}$ SXA with no affinity for the $D14^{-}E186^{-}$ form of SXA, but it is likely such inhibitors exist, just as it is likely that there are inhibitors that bind only to $D14^{-}E186^{-}$ SXA even though they are yet to be identified. Similar to substrates 4NPA and 4NPX, none of the four inhibitors show affinity for the catalytically inactive $D14^{H}E186^{H}$ SXA. The pH profiles for double-binding inhibitors, L-arabinose and D-ribose, indicate that the binding of a second equivalent of inhibitor occurs only with the $D14^{-}E186^{H}$ form of SXA, consistent with the view (and model of Fig. 1) that $D14^{-}E186^{-}$ SXA binds the first equivalent in a manner that prevents binding of the second equivalent from binding. A similar view holds for the formation of EIS: the $1/K_{is}$ term becomes insignificant at alkaline pH indicating that the $D14^{-}E186^{-}$ SXA cannot bind inhibitor and substrate simultaneously, whereas the $D14^{-}E186^{H}$ SXA can bind both simultaneously.

All inhibitor complexes defined by Scheme 1 have been exemplified by experiments in this work: EI (all inhibitors), EII (double binding of D-arabinose, L-arabinose, D-erythrose, and D-ribose), EIX (simultaneous binding by mixed inhibitor pairs L-arabinose/D-ribose, L-arabinose/D-xylose, and D-erythrose/D-ribose), and EIS (simultaneous binding by inhibitor/substrate pairs D-xylose/4NPX, L-arabinose/4NPA, L-arabinose/4NPX, D-erythrose/4NPA, D-erythrose/4NPX, L-xylose/4NPA, and L-xylose/4NPX). Among the nine monosaccharides studied in such detail, only D-glucose appears incapable of forming complexes beyond EI (EIS, EII and EIX complexes have not been demonstrated). It is interesting to speculate about the structural basis for limitation to single occupancy of the two-subsite active site: perhaps, D-glucose is too large to be accommodated by subsite −1 and it partially occupies subsite +1 so there is insufficient space remaining for binding a second ligand in subsite +1 or perhaps, D-glucose binds in a manner that prevents favorable interaction with a second ligand. Similar and additional possibilities may explain formation of some EII, EIS and EIX complexes and the lack of formation of others. In the case of L-arabinose, the initial weak complex of EII ($K_{i2(rapid)} \sim 300$ mM) isomerizes to a tighter complex ($K_{i2} \sim 100$ mM) that presumably involves movement of active-site residues or the sugar or both in finding a preferred orientation. Notably, the five-bladed β-propeller domain is considered a rigid structure capable of small changes [13].

Slow-binding, reversible inhibitors of enzymes are ordinarily associated with high affinity ligands [19,20], and this holds true for those that act on glycoside hydrolases [25]. In this sense, slow binding of L-arabinose is unusual because of its low affinity, but the phenomenon may be more common than recognized for several reasons. Perhaps the most prominent is that low affinity inhibitors have been inherently less interesting to enzymologists, particularly those pursuing improved effectiveness of enzyme inhibitors in applications such as ethical drugs and disease-control agents. As well, in the case of L-arabinose, the slow step is associated with binding of the second equivalent of inhibitor to the active site making the effect on enzyme activity more subtle and more easily overlooked. Whereas, binding of L-arabinose to SXA may be one of the weakest inhibitors known to display reversible slow binding inhibition, it has been instrumental in providing temporal dimension to the simultaneous binding of two inhibitors to SXA at equilibrium and, thereby, contributing further functional insight into the two-subsite model.

The mM binding constants, detailed in this work, gain significance of scale when SXA is applied to saccharification of herbaceous biomass (holocellulose) for subsequent fermentation to bioethanol where it is desirable to produce ~4 M ethanol. Thus, concentrations of monosaccharides can exceed 2 M comprising major constituents of D-glucose, D-xylose and L-arabinose (in most sources of holocellulose). Therefore, towards the end of saccharification, significant fractions of SXA would be complexed with monosaccharides and partitioned away from its hydrolase function. Natural substrates, xylooligosaccharides, are more efficiently hydrolyzed than 4NPX and 4NPA by SXA [3], and this would benefit saccharification efficiency. One means to avoid accumulation of inhibitory monosaccharides is by including the fermenting organism in the enzymatic saccharification reaction to drive the carbon flow towards ethanol; SXA is weakly inhibited by ethanol ($K_i = 1.04 \pm 0.08$ M at pH 7.0). Otherwise, structure–function definition of SXA-inhibitor complexes, described here, could lead to improved catalysts.

Acknowledgments

This work was supported by USDA funding of CRIS 3620-41000-118. The mention of firm names or trade products does not imply that they are endorsed or recommended by the U.S. Department of Agriculture over other firms or similar products not mentioned.

Appendix A. Supplementary data

Supplementary data associated with this article can be found, in the online version, at doi:10.1016/j.abb.2007.05.016.

References

[1] M.A. Cotta, T.R. Whitehead, Curr. Microbiol. 36 (1998) 183–189.
[2] T.R. Whitehead, M.A. Cotta, Curr. Microbiol. 43 (2001) 293–298.
[3] D.B. Jordan, X.-L. Li, C.A. Dunlap, T.R. Whitehead, M.A. Cotta, Appl. Biochem. Biotechnol. 141 (2007) 51–76.
[4] D.B. Jordan, X.-L. Li, C.A. Dunlap, T.R. Whitehead, M.A. Cotta, Appl. Biochem. Biotechnol. 136–140 (2007) 93–104.
[5] P.M. Coutinho, E. Deleury, B. Henrissat, J. Appl. Glycosci. 50 (2003) 241–244.
[6] B.C. Saha, J. Ind. Microbiol. Biotechnol. 30 (2003) 279–291.
[7] G.O. Aspinall, in: J. Preiss (Ed.), The Biochemistry of Plants, vol. 3, Academic Press, New York, 1972, pp. 473–500.
[8] L. Saulnier, C. Marot, E. Chanliaud, J.F. Thibault, Carbohyd. Polym. 26 (1995) 279–287.
[9] B.S. Dien, X.-L. Li, L.B. Iten, D.B. Jordan, N.N. Nichols, P.J. O'Bryan, M.A. Cotta, Enzyme Microb. Technol. 39 (2006) 1137–1144.
[10] K.A. Gray, L. Zhao, M. Emptage, Curr. Opin. Chem. Biol. 10 (2006) 141–146.
[11] B.S. Dien, N.N. Nichols, P.J. O'Bryan, R.J. Bothast, Appl. Biochem. Biotechnol. 84–86 (2000) 181–196.
[12] C. Brüx, A. Ben-David, D. Shallom-Shezifi, M. Leon, K. Niefind, G. Shoham, Y. Shoham, D. Schomburg, J. Mol. Biol. 359 (2006) 97–109.
[13] V. Fulop, D. Jones, T. Curr. Opin. Struct. Biol. 9 (1999) 715–721.
[14] D. Nurizzo, J.P. Turkenburg, S.J. Charnock, S.M. Roberts, E.J. Dodson, V.A. McKie, E.J. Taylor, H.J. Gilbert, G.J. Davies, Nat. Struct. Biol. 9 (2002) 665–668.
[15] F.J. Kezdy, M.L. Bender, Biochemistry 1 (1962) 1097–1106.
[16] S.C. Gill, P.H. von Hippel, Anal. Biochem. 182 (1989) 319–326.
[17] R.J. Leatherbarrow, Grafit Version 5, Erithacus Software Ltd., Horley, U.K., 2001.
[18] P.J. Marshall, M.L. Sinnott, Biochem. J. 215 (1983) 67–74.
[19] J.W. Williams, J.F. Morrison, Methods Enzymol. 63 (1979) 437–467.
[20] J.F. Morrison, C.T. Walsh, Adv. Enzymol. 61 (1988) 201–301.
[21] W.W. Cleland, Methods Enzymol. 87 (1982) 390–405.
[22] R. Wolfenden, X. Lu, G. Young, J. Am. Chem. Soc. 120 (1998) 6814–6815.
[23] M. Claeyssens, C.K. De Bruyne, Biochem. Biophys. Acta 533 (1978) 98–104.
[24] S.J. Angyal, Adv. Carbohyd. Chem. Biochem. 42 (1984) 15–68.
[25] G. Legler, Adv. Carbohyd. Chem. Biochem. 48 (1990) 319–384.